# Grid Performance of a V2G Capable EV Charger: A Case Study

Authored: Md Mejbaul Haque, Laura Jones, Kathryn Lucas-Healey, Bjorn Sturmberg

*This Project received funding from ARENA as part of ARENA's Advancing Renewables Program. The views expressed herein are not necessarily the views of the Australian Government, and the Australian Government does not accept responsibility for any information or advice contained herein*

# Contents

# Executive Summary

V2G, as described in [1] is a promising source of grid services. But as yet, the capability of V2G to provide this service at a technical level is unproven. This report aims to be a "first look" at this capability. It presents the results of a series of tests undertaken in the Australian National University (ANU) DERlab grid simulator facility. These tests were undertaken on a "Wallbox Quasar" charger between 10/2021 and 03/2022.

This suite of tests was undertaken as part of the Realising Electric Vehicle-to-Grid Services (REVS) project. This project tests V2G's capability to provide contingency frequency control ancillary services (FCAS) using a 51-vehicle fleet of EVs deployed across the Australian Capital Territory (ACT).

This report does not focus on FCAS – this is being validated as part of the trial. Instead, it aims to:

- Test the charger's performance against common grid conditions, using the AS4777.2:2020 requirements as a guide.
- Validate the charger's capability to provide additional services including reactive power, voltage control, and peak shaving.

The methodology and tests that have been performed to verify the charger's performance are presented in Section **2** and Section **3** respectively. It is important to note that the charger (wallbox quasar) unit that was used for these tests is a slightly earlier production unit that does not comply with AS4777.2:2020 due to hardware grounding issues however, the firmware is AS4777.2:2020 compliant. The performance of the charger against AS4777.2:2020 standard of the EV charger are presented in Section **4**. The detailed experimental test results are placed in **Appendix C**.

The tests in this report show that the charger's performance is adequate to meet the AS4777.2:2020 requirements. This indicates that the charger is likely to have adequate performance against most common grid disturbances. The charger is also complied with phase angle jump tests with variation of 60°±3° as stipulated in AS4777.2:2020. However, further tests and studies show that the charger does not ride through some phase angle jumps i.e. 45°. After 11 iterations of testing with 45° phase jump, it is found that the point of occurring phase angle jump on voltage waveform has a significant effect on the riding through behaviour.

It is important to remember that grid service performance of EV chargers is still developing. Services that require change in active power (such as peak shaving and some types of voltage management) are possible with the capabilities of the existing charger, although they are not

yet implemented by the JET charge controls. The reactive power control has not been implemented in charger's firmware. A summary of the test results is presented in **Table 1**. Results in this report must be taken in context of the charger's early stage of development. Performance is expected to improve over time as the manufacturer implements improvements.

**Table 1: Tests results**

| **Tests Cases** | **Performance against AS4777.2:2020** |
|---|---|
| Frequency response limit | **Complies** |
| Passive anti-islanding frequency limit | **Complies** |
| Passive anti-islanding voltage limit | **Complies** |
| Voltage limit for sustained operation | **Complies** |
| Voltage disturbance response | **Complies** |
| Rate of change in grid frequency (RoCoF) | **Complies** |
| Voltage phase angle jump/shift withstand capability | **Complies** |
| **Grid services** | **Charger capability** |
| Reactive power support | **Not implemented** |
| Voltage management | **Partially capable** |
| Peak shaving | **Capable** |

# 1. Introduction

## 1.1. Background

A bidirectional charger is a four-quadrant converter that allows charging and discharging of EV batteries, thereby enabling the provision of a range of grid services [2]. EV uptake is increasing, which will lead to a large number of vehicles throughout Australian power grids over the coming years. This creates scope for V2G to provide increasing amounts of grid services, and makes it all the more important to understand the performance of V2G during grid disturbances. In the REVS project, there will be 51 Nissan LEAF EVs deployed across Australian Capital Territory (ACT) to test and deliver frequency control ancillary services (FCAS) to the National Electricity Market (NEM). To facilitate FCAS, a total of 51 Wallbox bidirectional chargers having vehicle to grid (V2G) capability will be installed in ACT government facilities.

## 1.2. Purpose

The purpose of the document is to present experimental results of the EV charger under specific grid disturbances through a series of laboratory tests. The laboratory tests of the EV charger examines the following:

- Can the charger ride through common grid disturbances?
- Can the charger provide grid services?

# 2. Methodology

There are two types of tests undertaken in this study;

- Performance against AS4777.2:2020 requirements
- Grid services capability

AS4777 defines several types of grid conditions that the charger must ride through (or disconnect during). These are framed in terms of change in voltage and frequency over time. Voltage is a spatial variable because it changes across the power system based on its characteristics i.e., resistance, reactance, length and location. Frequency however is largely constant across a synchronous power system[1]. This means that voltage will change largely due to local disturbances, but a fault anywhere in the power system will alter frequency everywhere. Several research papers show that the operation of inverters is greatly impacted by grid events including unwanted frequency and voltage excursions [3, 4]. Therefore, examining the inverter's response to grid disturbances is necessary to understand if it complies with relevant connection standards.

In this report, voltage and frequency variables are used to simulate the different grid disturbances such as i) voltage disturbances, ii) frequency variation tests including rate of change of frequency (RoCoF), and iii) voltage phase-angle jumps. These disturbances are applied to a Wallbox quasar bidirectional EV charger rated to 7.4 kW and 32 A. This is an off-the shelf EV charger that has been certified to be AS 4777.2:2020 [5] compliant. It is important to note that quasar unit that was used for these tests is a slightly earlier production unit that does not comply with this Australian standard due to grounding issues. However, the firmware is AS4777.2:2020 compliant and its responses to voltage and frequency disturbances are expected to be same as the latest compliant hardware unit that is being currently manufactured.

Apart from the grid disturbances, there are emerging interests in evaluating V2G's capability to provide other ancillary services which are commonly termed as grid services. The grid services that V2G can provided additional to FCAS include peak shaving, load shifting, load levelling, valley filling, active and reactive power control, voltage and frequency regulation, and spinning reserve [6, 7]. In this report, the following additional grid services are explored.

- Reactive power control
- Voltage management

[1] In the NEM: South Australia, Victoria, New South Wales, Australian Capital Territory, and Queensland are the largest synchronous power system.

- Peak shaving

The experimental test system is shown in **Figure 1**. This is physically located at the DERlab at the Australian National University (ANU). A full 4-quadrant grid simulator is used to supply the bidirectional EV charger that connects the EV via CHAdeMO port.

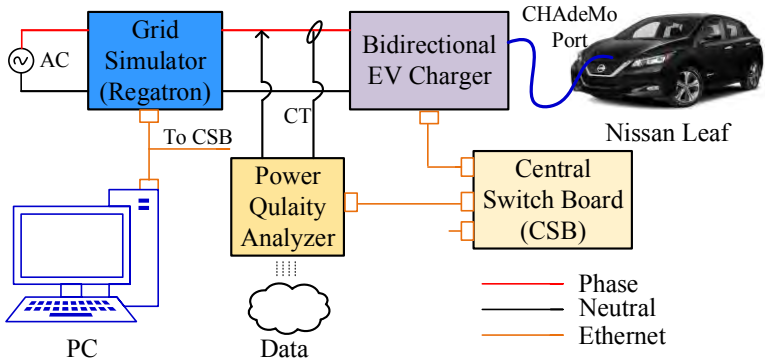


**Figure 1: Experimental test system.**

# 3. Test Performed

This series of experiments tested frequency response, passive anti-islanding, voltage, RoCoF, phase jumps, and active power management. Reactive power was not tested due to a lack of firmware support.

The frequency response limits and passive anti-islanding frequency limits in **Table 2** and **Table 3** are tested to investigate the frequency-watt response of the EV charger for an increase/decrease in frequency within the limits prescribed in AS4777.2:2020. The passive anti-islanding voltage limit tests in **Table 4** are carried out to observe the performance of EV charger for low voltage ride through and overvoltage. In addition to these voltage limit tests, the voltage limit for sustained operation and the response for grid voltage disturbances are tested as outlines in **Table 5** and **Table 6**.

Some inverters are very sensitive to the rate of change of frequency (RoCoF) and grid voltage phase angle jump/shift and cannot ride through these faults. The RoCoF, voltage phase angle jumps withstanding and active power control capabilities of the EV charger are tested as outlined in **Table 7** and **Table 9**.

The remarks columns in these tables represent the actual values of frequencies, voltages and phase angles used in these experimental tests. All these tests are performed with a Nissan LEAF EV. Initially, the EV keeps in idle state before testing starts and then energise the charger to charge/discharge the battery at full power of approximately ± 5.5 kW until disturbance is applied which is 20 s for frequency disturbance and 60 s for voltage disturbance tests. The frequency data is recorded using power meter. The accuracy of the measurement frequency data is 50 Hz (±0.1) in most cases.

The charger's responses to frequency, voltage disturbances and phase angle jumps are all consistent with AS4777.2:2020.

**Table 2: Frequency response limit**

| Test | Service | Frequency (Hz) | Remarks |
|---|---|---|---|
| Test 1 | Step rise in frequency | 50 to 52.05 Hz in different steps | 50.2 Hz, 50.3 Hz, 50.7 Hz, 50.8 z, 51 Hz, 51.5 Hz, 51.95 Hz |
| Test 2 | Step drop in frequency | 50 to 46.95 Hz in different steps | 49.8 Hz, 49.7 Hz, 49.05 Hz, 48.95 Hz, 48.5 Hz, 47.5 Hz, 47.05 Hz |

**Table 3: Passive anti-islanding frequency limit**

| Test | Service | Frequency (Hz) | Remarks |
|---|---|---|---|
| Test 1 | Under frequency 1 | < 47 Hz | 46.95 Hz |
| Test 2 | Over frequency 1 | > 52 Hz | 52.05 Hz |

**Table 4: Passive anti-islanding voltage limit**

| Test | Service | Voltage sags/rise (V) | Remarks |
|---|---|---|---|
| Test 1 | Undervoltage 1 | <180 V | 160 V |
| Test 2 | Undervoltage 2 | << 70 V | 65 V |
| Test 3 | Overvoltage 1 | >265 V | 272 V |
| Test 4 | Overvoltage 2 | >>275 V | 282 V |

**Table 5: Voltage limit for sustained operation**

| Test | Service | Maximum voltage (V) | Remarks |
|---|---|---|---|
| Test 1 | Voltage variations for sustained operation | 258 V | 258 V |

**Table 6: Voltage disturbance response**

| Test | Service | Voltage (V) | Remarks |
|---|---|---|---|
| Test 1 | Voltage disturbance withstanding capability | >260 V | 282 V |
| Test 2 | Voltage disturbance withstanding capability | 180 to 260 V | 230 V ->195 V->230 V |
| Test 3 | Voltage disturbance withstanding capability | <180V | 160 V |

**Table 7: Rate of change in grid frequency (RoCoF)**

| Test | Service | Frequency (Hz/s) | Remarks |
|---|---|---|---|
| Test 1 | RoCoF | 1 Hz/s | 50 Hz->51.95 Hz |
| Test 2 | RoCoF | 5 Hz/s | 50 Hz->55 Hz |

**Table 8: Voltage phase angle jump/shift withstand capability**

| Test | Service | Phase angle step (deg) | Remarks |
|---|---|---|---|
| Test 1 | Phase angle jump withstand | ±15° | ±15° |
| Test 2 | Phase angle jump withstand | ±30° | ±30° |

**Table 9: Active power control capability**

| Test | Service | Current limit (A) | Remarks |
|---|---|---|---|
| Test 1 | Charging | 25 A to 6 A | 15 A to 10 A |
| Test 2 | Discharging | − 25 A to – 6 A | -15 A to -10 A |

# 4. Performance of the charger against AS4777.2:2020

The purpose of these tests is to determine if the EV charger (multimode inverter as defined in AS4777.2:2020) remains connected at the extremes of the voltage, frequency and phase angle boundaries set out in AS4777.2:2020. These limits were tested using test profiles, described in **Appendix B**. The experimental tests and charger's performance are described in **Table 10** to **Table 12** for frequency, voltage and phase angle variables. More detailed test results are shown in **Appendix C**. For simplicity of understanding, the positive value of power indicates input power (vehicle charging) and negative power indicates output power (vehicle discharging) throughout this report. Also, for the sake of illustration, the EV charger is referred as "inverter" throughout this report unless otherwise specified.

**Table 10 Frequency variations tests: assessment**

| Tests | Aim of test | Assessment |
|---|---|---|
| Step rise in frequency | The aim of the tests is to verify that the multiple mode converter complies with the frequency limits specified in **Table 22** and **Table 23**. | **Complies** |
| Step drop in frequency | | |
| Under frequency 1 | The aim of the tests is to verify the under-frequency and over-frequency trip delay times and maximum disconnection times of the multiple mode inverter as specified in **Table 21**. | **Complies** |
| Over frequency 1 | | |
| RoCoF | The aim of the tests is to verify RoCoF withstanding capability of the multiple mode inverter as specified in **Table 30**. | **Complies** |

**Table 11 Voltage variations tests: assessment**

| Tests | Aim of test | Assessment |
|---|---|---|
| Under voltage 1 | The aim of the tests is to verify the undervoltage and overvoltage trip delay times and maximum disconnection times of the multiple mode inverter as specified in **Table 27.** | **Complies** |
| Under voltage 2 | | |
| Over voltage 1 | | |
| Over voltage 2 | | |
| Voltage limit for sustained operation | The aim of this test is to confirm the over-voltage limit ($V_{norm-max}$) for sustained operation as specified in **Table 28**. | **Complies** |
| Voltage disturbance withstanding capability | The aim of this test is to verify the inverter response in accordance with the voltage limits as specified in **Table 29**. | **Complies** |

**Table 12 Phase angle jump variations tests: assessment**

| Test | Aim of test | Assessment |
|---|---|---|
| Phase angle jump withstand | The aim of this test is to verify that the inverter complies with the voltage phase angle jump/shift requirement specified in **Table 31**. | **Complies** |

# 5. Grid Services additional to FCAS

Grid services include a suite of capabilities that can be used to support the power system. This group of tests assesses the capability of the charger to provide three services: Reactive power control, voltage management, and peak shaving services. Each mode is assessed by three capabilities:

- Is it implemented at a hardware level?
- Does the charger implement this capability in firmware?
- Does the JET charge aggregation platform support this capability?

These are described further below.

## 5.1. Reactive power support

Reactive power support is commonly used in voltage management services. Four-quadrant inverters can provide reactive power, and are used this way in the energy system commonly. Current-generation solar and battery inverters are commonly capable of providing this service as it meets the AS4777.2:2020 “Q-V mode” voltage control requirements and impacts active power minimally. At a hardware level, the vehicle-to-Grid (V2G) enabled charger is a four quadrant inverter. This means that at a hardware level the charger can provide reactive power support in the network while charging/discharging. Currently however the charger does not implement reactive power control at a firmware level. This includes the AS4777.2:2020 “Q-V” mode. Studies show that in constrained distribution grids, reactive power enhances coordinated charging and significantly reduces the average cost of charging [8, 9]. This allows more EVs to be integrated without violating the grid operating constraints. **Table 13** presents the assessment charger’s capability for reactive power support.

**Table 13 Assessment of reactive power control capability**

| Capability | Assessment |
|---|---|
| Hardware | **Capable** |
| Firmware | **Not implemented** |
| Aggregation | **Not implemented** |

## 5.2. Voltage management

Voltage management service is used to maintain power system voltage to within limits. This includes voltage rise problems during periods of high generation, or voltage drop when demand is high. In this situation, V2G chargers can assist managing voltage in two ways:

- Using reactive power control
- Using active power control

These control modes are defined (for management of local voltage) in AS4777 as “P-V” and “Q-V” modes. A voltage control service would extend this by aggregating several V2G chargers and controlling a remote voltage through an aggregation platform.

As described in **5.1**, the current Wallbox firmware does not implement and allow reactive power control. Active power control however is enabled and demonstrated in the REVS project – both during FCAS events and as part of compliance to dynamic operating envelopes. However remote voltage management is not currently implemented in the aggregation platform in use in this trial. The charger’s capability for network voltage management is presented in **Table 14**.

**Table 14 Assessment of voltage management capability**

| Capability | Assessment – Reactive power | Assessment – Active power |
|---|---|---|
| Hardware | **Capable** | **Capable** |
| Firmware | **Not implemented** | **Capable** |
| Aggregation | **Not implemented** | **Not implemented** |

## 5.3. Peak shaving

Peak shaving refers to the levelling-out of peaks in electricity demand by shifting some loads to off-peak periods. The objective is to avoid investment in generators or networks to supply peak demand. Peak demand occurs rarely, leaving these assets underutilised. It can be achieved through active power control in V2G capable chargers.

The Wallbox V2G charger can provide this service at a firmware level, and adjacent services (operating envelope management) are being implemented as part of the REVS trial. **Table 15** shows the charger’s capability to peak shaving service.

**Table 15 Assessment of peak shaving capability**

| Capability | Assessment |
|---|---|
| Hardware | **Capable** |
| Firmware | **Capable** |
| Aggregation | **Not implemented (but can be easily implemented)** |

# 6. References


[1] L. Jones, K. Lucas-Healey, B. Sturmberg, H. Temby and M. Islam, "The A to Z of V2G: A comprehensive analysis of vehicle-to-grid technology worldwide," Accessed on: March 8, 2021. [Online]. Available: https://arena.gov.au/assets/2021/01/revs-the-a-to-z-of-v2g.pdf.

[2] G. Buja, M. Bertoluzzo, and C. Fontana, "Reactive power compensation capabilities of V2G-enabled electric vehicles," *IEEE Trans. Power Electron.,* vol. 32, no. 12, pp. 9447-9459, 2017.

[3] K. Ndirangu, L. Callegaro, J. E. Fletcher, and G. Konstantinou, "Development of an Aggregation Tool for PV Inverter Response to Frequency Disturbances across a Distribution Feeder," in *IECON 2020 The 46th Annual Conference of the IEEE Industrial Electronics Society*, 2020, pp. 4037-4042.

[4] L. Callegaro, G. Konstantinou, C. A. Rojas, N. F. Avila, and J. E. Fletcher, "Testing Evidence and Analysis of Rooftop PV Inverters Response to Grid Disturbances," *IEEE Journal of Photovoltaics,* vol. 10, no. 6, pp. 1882-1891, 2020.

[5] *Grid Connection of Energy Systems via Inverters. Part 2: Inverter Requirements*, Standards Australia/Standards New Zealand Std. AS/NZS 4777.2, 2020.

[6] T. S. Ustun, A. Zayegh, and C. Ozansoy, "Electric Vehicle Potential in Australia: Its Impact on Smartgrids," *IEEE Industrial Electronics Magazine,* vol. 7, no. 4, pp. 15-25, 2013.

[7] N. Erdogan, F. Erden, and M. Kisacikoglu, "A fast and efficient coordinated vehicle-to-grid discharging control scheme for peak shaving in power distribution system," *Journal of Modern Power Systems and Clean Energy,* vol. 6, no. 3, pp. 555-566, 2018/05/01 2018.

[8] J. Wang, G. R. Bharati, S. Paudyal, O. Ceylan, B. P. Bhattarai, and K. S. Myers, "Coordinated Electric Vehicle Charging With Reactive Power Support to Distribution Grids," *IEEE Transactions on Industrial Informatics,* vol. 15, no. 1, pp. 54-63, 2019.

[9] S. Paudyal, O. Ceylan, B. P. Bhattarai, and K. S. Myers, "Optimal coordinated EV charging with reactive power support in constrained distribution grids," in *2017 IEEE Power & Energy Society General Meeting*, 2017, pp. 1-5.

[10] E. van der Vleuten and V. Lagendijk, "Transnational infrastructure vulnerability: The historical shaping of the 2006 European Blackout," *Energy Policy,* vol. 38, no. 4, pp. 2042-2052, 2010.

[11] *Grid Connection of Energy Systems via Inverters. Part 2: Inverter Requirements*, Standards Australia/Standards New Zealand Std. AS/NZS 4777, 2015.

[12] *Grid Connection of energy systems via inverters, Part 2: Inverter requirements*, Standards Australia/Standards New Zealand Std. AS/NZS 4777, 2005.

[13] L. Yao, X. Xiao, Y. Wang, and W. Xu, "Adaptive Contactor - A New Scheme to Improve Induction Motor Immunity to Voltage Sags," *IEEE Transactions on Power Delivery,* pp. 1-1, 2020.

[14] D. Llanos *et al.*, "Classification of short duration faults (voltage sags) in transmission and distribution power systems," in *2003 European Control Conference (ECC)*, 2003, pp. 1246-1251.

[15] M. Coumont, F. Bennewitz, and J. Hanson, "Influence of Different Fault Ride-Through Strategies of Converter-Interfaced Distributed Generation on Short-Term Voltage Stability," in *2019 IEEE PES Innovative Smart Grid Technologies Europe (ISGT-Europe)*, 2019, pp. 1-5.

[16] L. Su, X. Qin, Y. Jiang, Y. Zhang, J. Wu, and Y. Han, "Study on the Definition and Performance of Fast Frequency Response from Inverter-Based Resources," in *2020 IEEE/IAS Industrial and Commercial Power System Asia (I&CPS Asia)*, 2020, pp. 1388-1395.

[17] B. Kroposki *et al.*, "Achieving a 100% Renewable Grid: Operating Electric Power Systems with Extremely High Levels of Variable Renewable Energy," *IEEE Power and Energy Magazine,* vol. 15, no. 2, pp. 61-73, 2017.

[18] D. Pattabiraman, J. Tan, V. Gevorgian, A. Hoke, C. Antonio, and D. Arakawa, "Impact of Frequency-Watt Control on the Dynamics of a High DER Penetration Power System," in *2018 IEEE Power & Energy Society General Meeting (PESGM)*, 2018, pp. 1-5.

[19] A. Luna, U. Tamrakar, T. M. Hansen, and R. Tonkoski, "Frequency Response in Grids with High Penetration of Renewable Energy Sources," in *2018 North American Power Symposium (NAPS)*, 2018, pp. 1-5.

# Appendix A Background

## A.1 Background Studies

Electric vehicles (EVs) are generally connected to the electricity network through off-the-shelf chargers. Chargers can be unidirectional or bidirectional. The bidirectional (V2G) chargers can enable EV batteries to discharge as well as charge. This V2G service is an emerging technology that is being developed because it allows higher utilisation of EV batteries. This promises financial and non-financial benefits for stakeholders such as EV owners, electricity system and wider communities, as described in [1].

For these contributions to be valuable, it is critical that grid operators properly understand the behaviour of bidirectional EV chargers under grid disturbances. Successful service delivery requires the charger remain connected during disturbances. The embedded firmware of these chargers will determine their response to grid disturbances and compliance with technical standards. These standards are prepared based on extensive investigation of inverter operations and the impact of inverter failure due to grid disturbances. Inverter grid support modes were implemented in standards in the past decade to provide grid support outside the normal operating band of the inverters. Some recent blackouts, such as the European blackout in 2006, have caused severe frequency disturbances and led to grid instabilities [10]. Following this event, the inverter frequency-watt response mode is now included in many technical standards, including AS/NZS 4777.2:2015, to provide droop control of inverter output power at increased frequencies [11]. This mode prevents the inverter's disconnection from the grid at a fixed frequency threshold and prevents the loss of renewable generation. It also increases the operating range of the inverter interfaced renewable generation. This standard also stipulate that the grid-connected PV inverters must have voltage control modes for voltage regulation. There are two main types of voltage control modes: active power curtailment and reactive power control. Active power curtailment mode causes the inverter to reduce PV export power in response to voltage rise. The reactive power control mode allows the inverter to absorb or supply reactive power to regulate an over or under voltage problem on the network. Similar standards and device performances are not yet in place for EV chargers. However, vehicle-to-grid (V2G) capable electric vehicle supply equipment such as bidirectional EV chargers are covered by the current AS/NZS 4777.2:2020 standard, which treats them as multiple mode inverters because they have charging and discharging modes [5].

**Introducing the Realising Electric Vehicle-to-grid Services (REVS) trial**

This report has been developed as part of the REVS trial. In an Australian first, the Realising Electric Vehicles-to-grid Services (REVS) project demonstrates how commercially available electric vehicles (EVs) and chargers can contribute to energy stability by transferring power back and forth into the grid, as required.

EVs will inject power back into the grid during rare events (to avoid possibility of blackouts) and EV owners will be paid when their vehicles are used for this service.

Employing 51 Nissan LEAF EVs across the ACT as part of the ACT government and ActewAGL fleet, the REVS project seeks to support the reliability and resilience of the electricity grid, unlocking economic benefits making electric vehicles a more viable and appealing transport option for fleet operators.

The REVS consortium covers the whole electricity and transport supply chains including ActewAGL, Evoenergy, Nissan, SG Fleet, JET Charge, ACT Government and the Australian National University. Together the consortium will produce a roadmap with recommendations that will accelerate the deployment of V2G nationally.

The project has been endorsed by the Australian Renewable Energy Agency (ARENA) and has received funding as part of ARENA's Advancing Renewables Program.

REVS is underway and will publish a final report in late 2022.

https://secs.accenture.com/accenturems/revs/

## A.2 Single line diagram of ANU DERlab

**Figure 2** shows the single-line diagram (SLD) of the ANU DERlab. The EV charger will be connected at the connection point 1 (CP 1) to perform the test. These connection points can be directly connected to the evoenergy network or to the grid simulator.

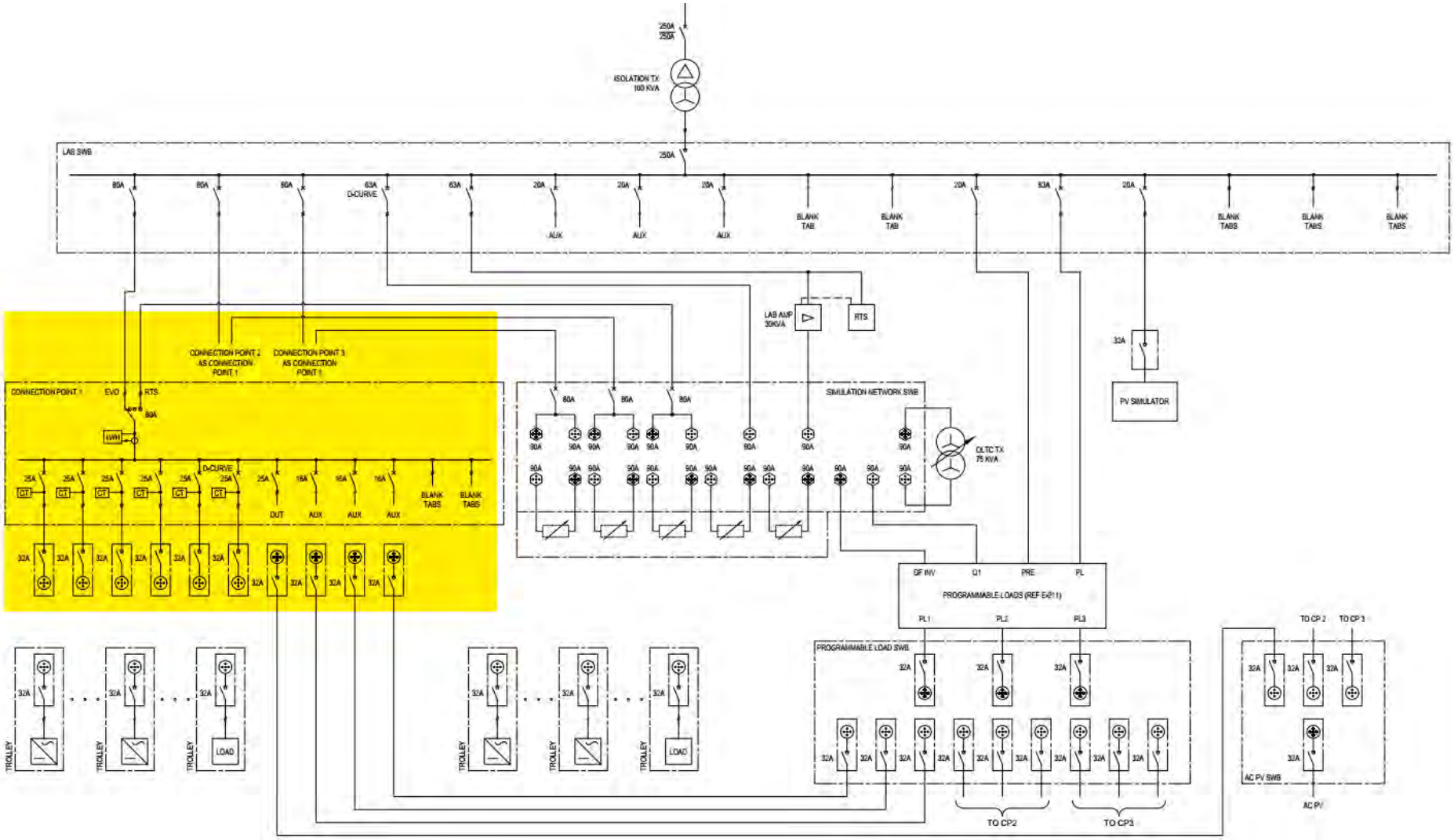


**Figure 2: Single-line diagram of ANU DERlab**

## A.3 Experimental test set-up

The laboratory setup of the EV charger in the ANU DERlab is shown in **Figure 3**. The laboratory setup comprises of a grid simulator, a V2G capable "Wallbox Quasar" EV charger mounted on a pole, a Nissan LEAF EV with CHAdeMO port and measurement devices. The technical specifications of the EV and hardware used for laboratory testing are presented below:


**Figure 3: EV charger's testing setup in the ANU DERlab.**

### A.3.1 V2G capable wallbox quasar

Wallbox quasar is a DC bidirectional EV charger to directly charge and discharge the EVs through its CCS or CHAdeMO port. The charger is generally controlled using the Wallbox App. The technical specification is shown in **Table 16**.

**Table 16 Technical specifications of wallbox quasar**

| | |
|---|---|
| **Manufacturer** | Wallbox |
| **Model** | DC charger |
| **Connector type** | CCS or CHAdeMO |
| **Maximum power** | 7.4 kW (single phase) |
| **AC voltage** | 230 V AC ±10% |
| **DC voltage** | 150 V – 500 V |
| **Maximum current** | 32 A (Charging current configurable from ± 6 A to ± 32 A) |
| **Rated frequency** | 50 Hz |

### A.3.2 Nissan LEAF

The specification of the Nissan LEAF EV is shown in **Table 17**.

**Table 17 Technical specifications of 2021 white Nissan LEAF sedan**

| | |
|---|---|
| **Manufacturer** | Nissan |
| **Model** | 2021 WHITE NISSAN SEDAN |
| **Battery** | |
| **Type** | Laminated lithium ion |
| **Voltage** | 350 V |
| **Capacity** | 40 kWh |
| **Charging** | |
| **On-board charger** | 6.6 kW |
| **CHAdeMO port** | 50 kW |
| **Charging time (6.6 kW on-board charger)** | Around 7.5 hrs to charge from alert to 100% at 32 A |
| **Charging time (50 kW rapid charger)** | Around 60 min to charge from 20% to 80%. (charging time is dependent on charging conditions, including charger type and condition, battery temperature as well as ambient temperature at point of use) |

### A.3.3 Grid simulator

The frequency disturbance will be created using the Regatron grid simulator at ANU DER Lab. During the duration of contingency FCAS test, the bi-directional charger will be responsive to the signal created by this grid simulator. The technical parameters of the Regatron grid simulator is given in **Table 18**.

**Table 18 Technical specifications of Regatron grid simulator**

| | |
|---|---|
| **Manufacturer** | Regatron |
| **Model** | TC.ACS.30.528.4WR.S.LC |
| **AC lineside ratings** | |
| **Line voltage** | 3 x 360 – 528 VAC |
| **Line frequency** | 48 – 62 Hz |
| **Input current** | 3 x 54 Arms |
| **AC loadside ratings** | |
| **Power range** | 0-30 kVA |
| **Voltage range** | 0 – 305 Vrms (L-N) |
| Frequency range | 0 – 1000 Hz |
| Current range | 3 x 0 – 43 A |

### A.3.4 Power meter

The key parameters of assessing the tests capabilities are the active and reactive power flow between the grid and the EVs. Thus, the active and reactive power at the connection points (1 or 2 or 3) in DER Lab will be recorded for each test. Furthermore, for the verification of frequency measurement capabilities within the defined conditions as well as for post-test analysis, grid frequency will be measured at the connection point. The technical specification of the SATEC power meter is presented in **Table 19**. Further measurement accuracy details are shown in
**Table 20**.

**Table 19 Technical specifications of SATEC power meter**

| | |
|---|---|
| **Manufacturer** | SATEC |
| **Model** | eXpertPRO DIN EM3250 |
| **Power supply** | |
| **Rated input:** | 85-332VAC 50/60Hz, 40-290VDC |
| **Over-voltage withstands:** | 1000 VAC continuous, 2000 VAC for 1 second |
| **Voltage inputs** | |
| **Operating range** | 10VAC (L-L) to 1000VAC (L-L) |
| **Current inputs** | |
| **Magnitude** | 1A-5A secondary (standard) |
| **Operating range** | continuous 10A RMS |
| **Overload withstands** | 15A RMS continuous, 200A (25 x Imax) RMS for ½ second |
| **Sampling rate** | 256 samples/cycle |

For the purpose of post-test analysis, other parameters as given below may need to be recorded at the connection point.

- Voltage
- Current
- Power factor
- Reactive power

**Table 20 Measurement accuracy details of the power meter (EM3250)**

| Parameter | Full Scale @ Input Range | Accuracy | | | Range |
|---|---|---|---|---|---|
| | | % Reading | % FS | Conditions | |
| Voltage | 120VxPT @ 120V<br>400VxPT @ 690V | 0.1 | 0.02 | 10% to 120% FS | 0 to 1,150,000 V<br>Starting voltage 1.5-5.0% FS (selectable) |
| Line current | CT | 0.1 | 0.02 | For In = 5A 1% to 200% FS<br>For In = 1A 5% to 200% FS | 0 to 50,000 A<br>Starting current 0.1% FS |
| Active power | 0.36×PT×CT @ 120V<br>1.2×PT×CT @ 690V | 0.2 | 0.02 | \|PF\| ≥ 0.5 | -10,000,000 kW to +10,000,000 kW |
| Reactive power | 0.36×PT×CT@ 120V<br>1.2×PT×CT @ 690V | 0.2 | 0.04 | \|PF\| ≤ 0.9[1] | -10,000,000 kvar to +10,000,000 kvar |
| Apparent power | 0.36×PT×CT @ 120V<br>1.2×PT×CT @ 690V | 0.2 | 0.02 | \|PF\| ≥ 0.5[1] | 0 to 10,000,000 kVA |
| Power factor | 1.000 | | 0.2 | \|PF\| ≥ 0.5, I ≥ 2% FSI | -0.999 to +1.000 |
| Frequency | | 0.002 | | VL-N > 25V | 40 Hz to 70 Hz |
| Total Harmonic Distortion, THD V (I), %Vf (%If) | 999.9 | 1.5 | 0.2 | THD ≥ 1%, V ≥ 10% FSV and $V_{L-N}$ > 25V, I ≥ 10% FSI | 0 to 999.9 |
| Total Demand Distortion, TDD, % | 100 | | 1.5 | TDD ≥ 1%, I ≥ 10% FSI, $V_{L-N}$ > 25V | 0 to 100 |
| Active energy Import & Export | | Class 0.2S under conditions as per IEC 62053-22:2003 | | | 0 to 999,999,999 kWh |
| Reactive energy Import & Export | | Class 0.5S under conditions as per IEC 62053-24:2015 | | | 0 to 999,999,999 kvarh |
| Apparent energy | | Class 0.2S under conditions as per IEC 62053-22:2003 | | | 0 to 999,999,999 kVAh |

### A.3.5 Software Interface

The software for grid simulator is installed in the computer to change set points and to interface with the grid simulator. The software interface is shown in **Figure 4**. This is used to define the appropriate modulation and set points to produce the desired test profiles for generating common grid disturbances including step frequency variations, voltage sags, RoCoF and phase angle jumps. The below disturbances are considered and applied for the tests:

1) Step frequency changes

2) Voltage sag

3) Rate of change of frequency

4) Frequency notch

5) Phase angle jumps

The following algorithm is implemented in the software to produce the grid disturbances, i.e., voltage and frequency variations:

Step 1: Run the grid simulator control interface and adjust the parameters of the ac grid simulator to required set-points.

Step 2: Generate desired disturbance/test profiles using appropriate modulation method.

Step 3: Subject the EV charger to the disturbances through the grid simulator software.

Step 4: Record voltage, current, frequency and power data for post analysis to interpret the behaviour of EV charger.

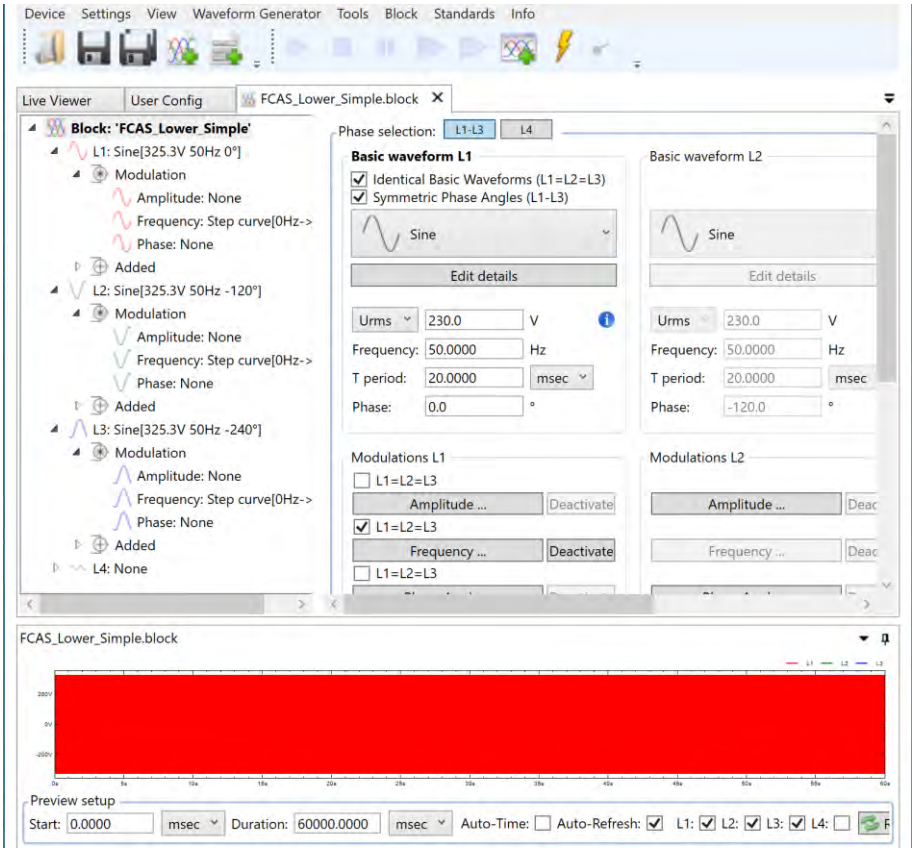


**Figure 4: ACS control interface of a grid simulator interface.**

The rms voltage and current values are recorded by a power meter. The active and reactive power are calculated at the post-processing stage using the power meter data. The experimental data can also be captured by the point-on-wave meter operating at 62 kHz and post analysed. The point-on-wave meters with associated display allow users to visualise real-time measurement data and waveforms directly.

# Appendix B Test Profiles

## B.1 Frequency variations

The Australian standards set the frequency boundaries and thus impose the upper and lower limits within which the inverter must remain connected with the ac grid. For example, these frequency boundaries are defined as 45 Hz < f < 55 Hz and 47 Hz < f < 52 Hz by the previous standards, i.e., AS/NZS 4777.3:2005 [12] and AS/NZS 4777.2:2015 [11] respectively. These frequency limits need to be verified by experimental tests to ensure that the EV charger remains connected within the specified frequency range while it maintains output power according to the frequency-watt characteristics. An example test profile of step frequency changes is shown in **Figure 5** which is applied on the AS/NZS 4777.2:2020 compliant EV charger to test its behaviour.

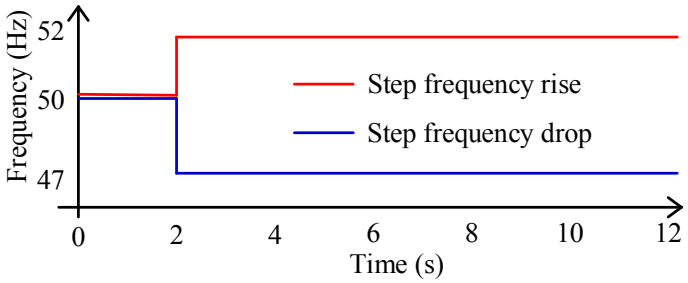


**Figure 5: An example test profile of step frequency variations.**

**Table 21 Passive anti-islanding frequency limit values** [5]

| | Region | Australia A |
|---|---|---|
| Under-frequency 1 (F<) | Protection function limit value | 47 Hz |
| | Trip delay time | 1 s |
| | Maximum disconnection time | 2 s |
| Over-frequency 1 (F>) | Protection function limit value | 52 Hz |
| | Trip delay time | - |
| | Maximum disconnection time | 0.2 s |

**Table 22 Frequency variation withstand limits** [5]

| Inverter response | Decrease in frequency response Lower limit (Hz) | Lower limit of continuous operation range ($f_{LLCO}$) (Hz) | Upper limit of continuous operation range ($f_{ULCO}$) (Hz) | Increase in frequency response Upper limit (Hz) |
|---|---|---|---|---|
| Range | - | 49.5 – 49.9 | 50.1 – 50.5 | - |
| Australia A | 47 | 49.75 | 50.25 | 52 |

**Table 23 Frequency response limits** [5]

| Inverter response | Decrease in frequency response limit (Hz) | | Increase in frequency response limit (Hz) | |
|---|---|---|---|---|
| | Frequency where power output level is maximum ($f_{Pmax}$) (Hz) | Frequency where charging power level is zero ($f_{stop-ch}$) (Hz) | Frequency where discharging power level is zero ($f_{transition}$) (Hz) | Frequency where power level is minimum ($f_{Pmin}$) (Hz) |
| Range | 47 to 49 | 48 – 49.5 | 50.5 – 52 | 51 to 53 |
| Australia A | 48 | 49 | 50.75 | 52 |

**Table 24 Frequency response – maximum completion time** [5]

| Region | Response commencement time | Response completion time |
|---|---|---|
| All | 1 s | 10 s |

### B.1.1 Frequency-watt response for inverter with energy storage (EV charger)

The EV charger is classified as multiple mode converter in AS4777.2:2020 [5]. The frequency response of the EV inverter with battery storage is presented in this section. **Figure 6** shows a two stage frequency response for an increase in frequency for the EV charger (multiple mode inverter with energy storage) for $f_{transition}$ of 50.75 Hz. **Figure 7** shows a two stage frequency response for a decrease in frequency for the EV charger (multiple mode inverter with energy storage) for $f_{stop-ch}$ of 49.0 Hz.

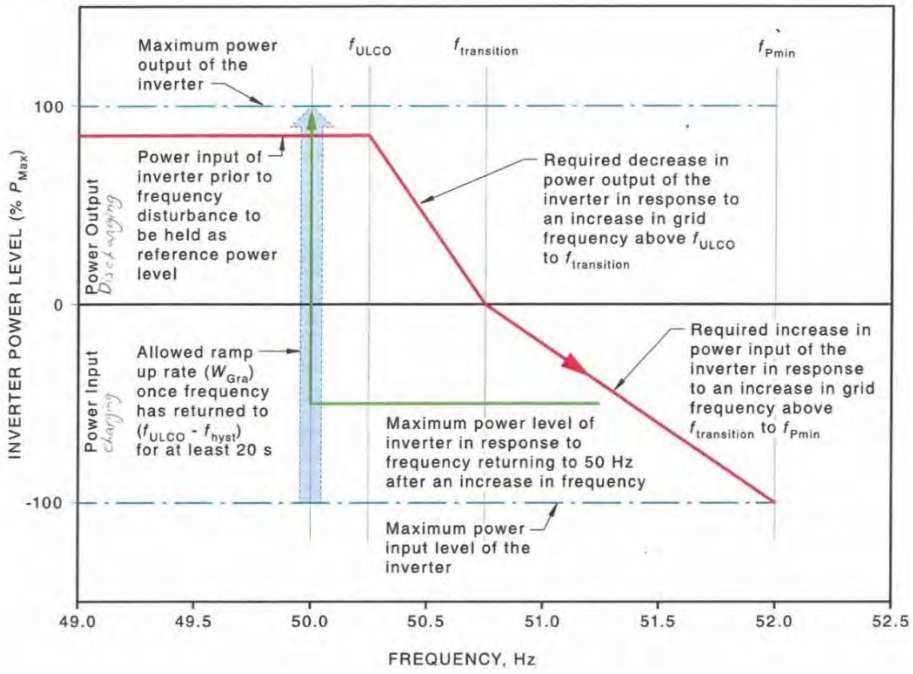


**Figure 6 Frequency response for an increase in frequency for the EV charger (multiple mode inverter with energy storage) for $f_{transition}$ of 50.75 Hz [5].**

**Table 25 Multiple mode inverter frequency response for an increase in frequency** [5]

| Conditions | Multiple mode inverter response |
|---|---|
| $f_{dist} > f_{ULCO}$ and battery is discharging through grid interactive port by multiple mode inverter. | The inverter shall reduce the power output linearly with the increase in frequency until $f_{transition}$ is reached. |
| $f_{dist} > f_{ULCO}$ and battery is charging from grid interactive port by multiple mode inverter. | The inverter shall maintain at least the same power input level with the increase in frequency until $f_{transition}$ is reached. |
| $f_{dist} = f_{transition}$ | The inverter power output shall be ceased (i.e. 0 W) |
| $f_{dist} > f_{transition}$ | The inverter shall increase the power input level through the grid interactive port linearly with the increase in frequency until $f_{Pmin}$ is reached, the maximum discharge rate of the battery is reached or the SOC of the battery is full. |
| $f_{dist}$ is between $f_{ULCO}$ and $f_{transition}$ | The inverter power level shall remain at or below the lowest power output level. |
| $f_{dist}$ is between $f_{transition}$ and $f_{Pmin}$ | The inverter power level shall remain at or above the highest power input level unless the SOC of the battery is full. |

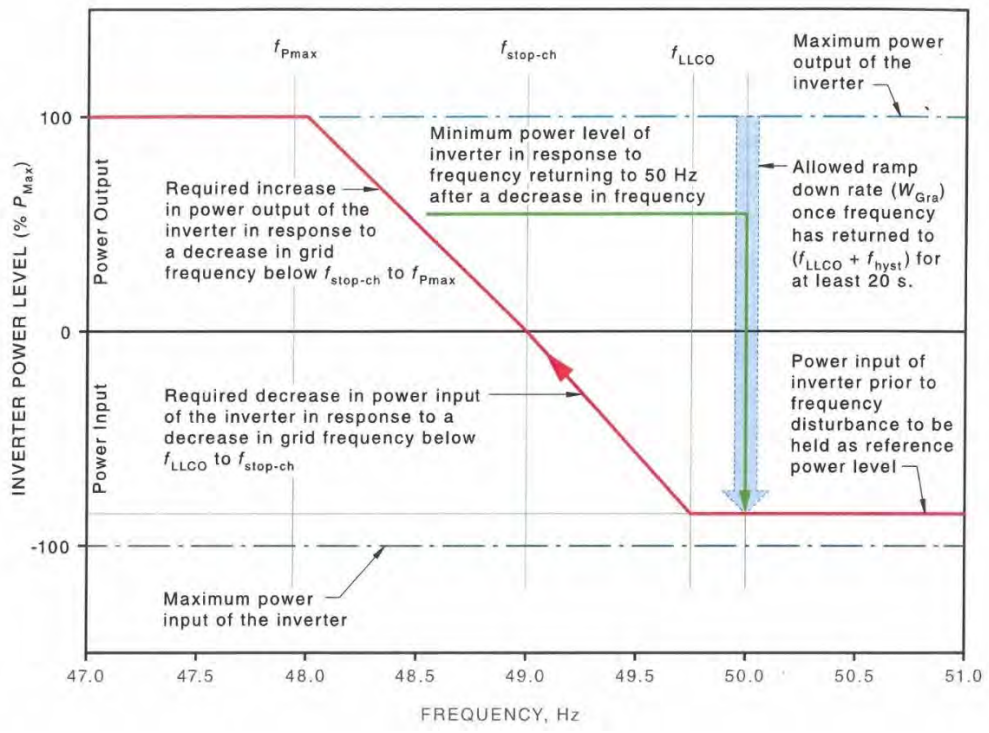


**Figure 7 Frequency response for a decrease in frequency for the EV charger (multiple mode inverter with energy storage) for $f_{stop-ch}$ of 49.0 Hz [5].**

**Table 26 Multiple mode inverter frequency response for a decrease in frequency** [5]

| Conditions | Multiple mode inverter response |
|---|---|
| $f_{dist} < f_{LLCO}$ and battery is discharging through grid interactive port by multiple mode inverter. | The inverter shall maintain at least the same power output level until $f_{stop-ch}$ |
| $f_{dist} < f_{LLCO}$ and battery is charging from grid interactive port by multiple mode inverter. | The inverter shall reduce input power level linearly with decrease in frequency until $f_{stop-ch}$ is reached. |
| $f_{dist} = f_{stop-ch}$ | The inverter shall have ceased charging the battery via grid interactive port (i.e. 0 W) |
| $f_{dist} < f_{stop-ch}$ | The inverter shall increase the power output level through the grid interactive port linearly with the decrease in frequency until $f_{Pmax}$ is reached, the maximum discharge rate of the battery is reached or the SOC of the battery is exhausted. |
| $f_{dist}$ is between $f_{LLCO}$ and $f_{stop-ch}$ | The inverter power level shall remain at or below the lowest power input level. |
| $f_{dist}$ is between $f_{stop-ch}$ and $f_{Pmax}$ | The inverter power level shall remain at or above the highest power output level. |

## B.2 Voltage sags

Voltage sags are defined as the reduction in rms grid voltage for a short duration that might occur due to short circuit faults, feeder overloading or starting of large inductive motor loads in the electricity grid [13]. During voltage sags, the rms value of the grid voltage might fall to 10% to 90% of the nominal grid voltage for a few milliseconds to several seconds [14]. The voltage sags might cause undesirable behaviour of the power electronics inverters that connect DERs into the grid. It is important that the operation of the EV chargers are tested in response to voltage sags against the current standard AS/NZS 4777.2:2020 [5]. The current standard sets the limits of undervoltages in two categories, i.e., undervoltage 1 (V<70) and undervoltage 2 (V<180) while the overvoltages limits are overvoltage 1 (V>265) and overvoltage 2 (V>275) [5]. It is expected that the EV charger should continue its operation with reduced power if the voltage sags are within 180<V<265 and should recover to pre-disturbance power level once the grid voltage returns back to nominal grid voltage (230V) [15]. However, the EV charger might disconnect if the voltage sags are beyond the voltage boundaries (180<V<265) and these voltage sag disturbances last for more than trip delay time which is 10 s for undervoltage 2 as defined in the new standard [5]. An example test profile of voltage sag is shown in **Figure 8**.

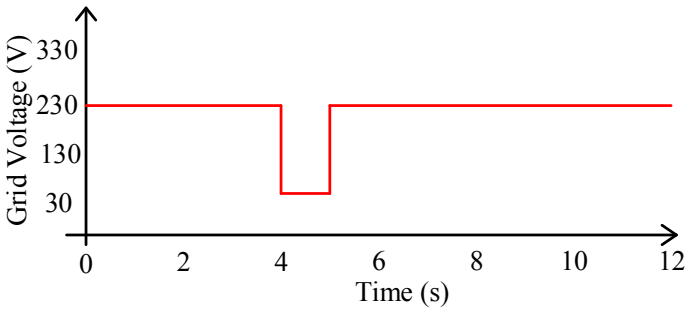


**Figure 8: An example test profile of voltage sag.**

**Table 27 Passive anti-islanding voltage limit values** [5]

| Protection function | Protection function limit | Trip delay time | Maximum disconnection time |
|---|---|---|---|
| Undervoltage 2 (V<<) | 70V | 1 s | 2 s |
| Undervoltage 1 (V<) | 180V | 10 s | 11 s |
| Overvoltage 2 (V>>) | 265V | 1 s | 2 s |
| Overvoltage 1 (V>) | 275V | - | 0.2 s |

**Table 28 Settings for ($V_{norm-max}$)** [5]

| Region | Default set point |
|---|---|
| Australia A | 258 V |

**Table 29 Voltage disturbance response** [5]

| Voltage limits | Inverter response |
|---|---|
| >260 V | Cease power generation |
| 180 V to 260 V | Continuous operation |
| <180 V | Cease power generation |

## B.3 RoCoF

The rate of change of frequency (RoCoF) is the ramp rate of grid frequency changes in response to mismatch of generation and demand power that might be caused due to the sudden loss of generators or loads [16]. This causes the grid frequency to deviate from its steady state operating points at nominal value (50 Hz). The deviation of the grid frequency occurs linearly between two different steady state points instead of an abrupt change from the nominal frequency of 50 Hz. It is very important to resist this linear deviation in grid frequency to maintain the power system operation within the stability limit that requires enough system inertia. Inertia is a factor that determines the ability of a power system to ride through frequency deviations while maintaining the stable grid frequency [17]. Low inertia systems may have very high RoCoF after an event, causing large frequency swings. Power systems are experiencing high levels of penetration of inverter interfaced generation in distribution networks through DERs such as PV systems, battery energy storage systems (BESS), and electric vehicles. These inverters both usually offer no inertia and are may disconnect during high RoCoF events, causing loss of generation [18]. It is critical inverters ride through high RoCoF events. Similarly, DERs should actively participate in contingency frequency support in response to partially mitigate the low inertia problems [19]. The current AS/NZS 4777.2:2020 standard prescribes that the inverters must be connected within the boundaries of 47 Hz < f < 52 Hz and should regulate the output power according to a frequency-watt response curve [5]. An example test profile of +1 Hz/s RoCoF is shown in **Figure 9**. This test profile was applied to the EV charger in order to evaluate its response.

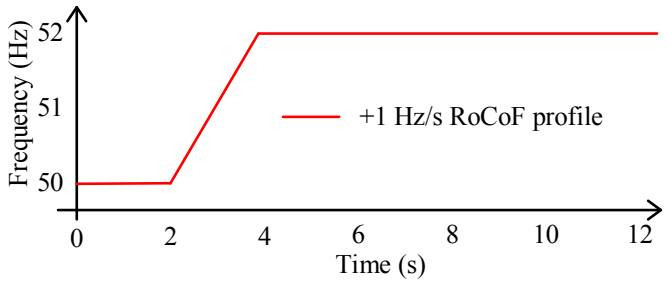


**Figure 9: An example test profile of +1 Hz/s RoCoF.**

**Table 30 Rate of change of frequency** [5]

| RoCoF (Hz/s) | Duration | Inverter response |
|---|---|---|
| ±1 Hz/s to ±4 Hz/s | 0.25 s | Continuous operation |
| >±4 Hz/s | - | Cease power generation |

## B.4 Frequency notch

**Figure 10** shows an example test profile for frequency notch.

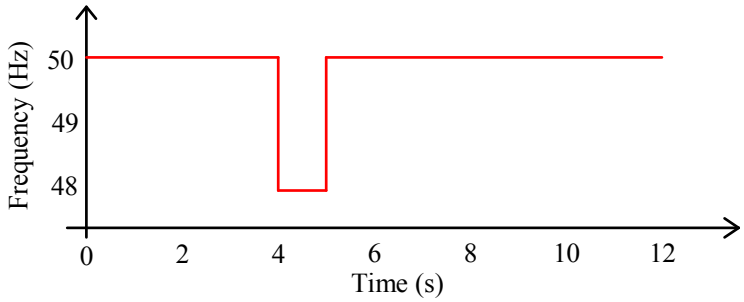


**Figure 10: An example test profile of frequency notch.**

## B.5 Phase angle jumps

**Figure 11** shows an example test profile of phase angle jump.

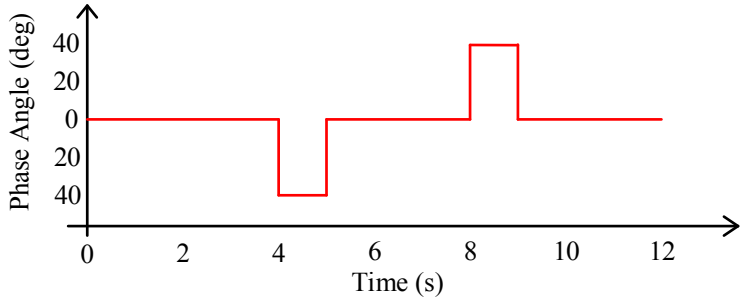


**Figure 11: An example test profile of phase angle jump (-40° to 40°).**

**Table 31 Voltage phase angle jump/shift withstand requirements** [5]

| | Single phase disturbance | Three phase disturbance |
|---|---|---|
| Single phase inverter | 60° | - |
| Three phase inverter | 60° | 20° |

# Appendix C Experimental Test Results

## C.1 Test results for frequency variables

**Table 32 Frequency variations tests: success criteria**

| Tests | Aim of test | Success criteria |
|---|---|---|
| Step rise in frequency<br>Step drop in frequency | The aim of the tests is to verify that the multiple mode converter complies with the frequency limits specified in **Table 22** and **Table 23**. | (i) The inverter shall maintain continuous operation for frequency variations within the limits specified in<br>(ii) **Table 22** and respond as defined in **Table 23**.<br>(iii) The inverter should respond to a variation of grid frequency as specified in **Table 25** and **Table 26**.<br>(iv) The inverter should stabilise the power level after a frequency disturbance within the response completion time as specified in **Table 24**.<br>(v) The inverter should maintain continuous operation for a RoCoF event as specified in **Table 30**. |
| Under frequency 1<br>Over frequency 1 | The aim of the tests is to verify the under-frequency and over-frequency trip delay times and maximum disconnection times of the multiple mode inverter as specified in Table 21. | (i) For sustained variation in frequency beyond each limit specified in **Table 21**, the automatic disconnection device shall operate no sooner than the required trip delay time and before the maximum disconnection time.<br>(ii) The inverter shall remain in continuous operation for frequency variations with a duration shorter than the trip delay time as specified in **Table 21**. |
| RoCoF | The aim of the tests is to verify RoCoF withstanding capability of the multiple mode inverter as specified in **Table 30**. | (i) The inverter shall maintain continuous operation for frequency excursions with a RoCoF of up to ± 4 Hz/s for a duration of 0.25 s. |

### C.1.1 Frequency response limits: Step rise in frequency

In this test, an incremental increase in grid frequencies is created by the grid simulator to verify the frequency-watt response of the inverter in different frequency values from 50 Hz to 52 Hz.

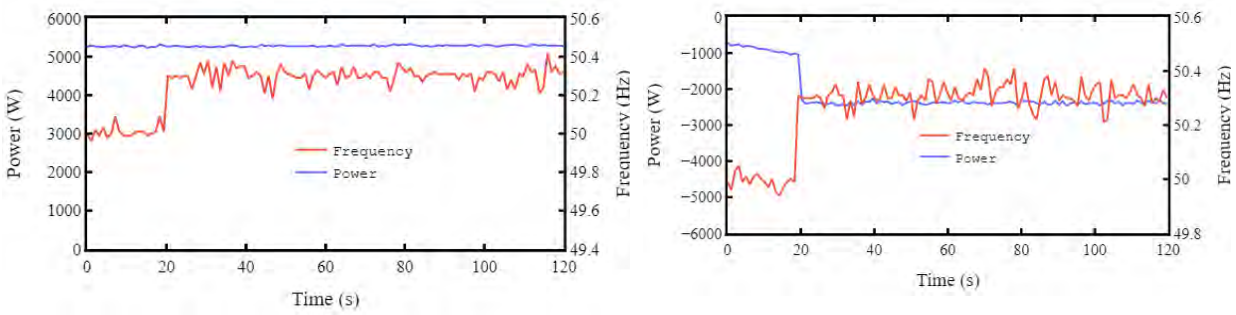


(a) (b)

**Figure 12: Frequency-watt response for step rise in frequency from (50 Hz to 50.30 Hz) (a) charging (b) discharging.**

**Figure 12** shows the frequency-watt response of the inverter for a step rise in frequency from 50 Hz to 50.30 Hz that exceeds $f_{ULCO}$ but below $f_{transition}$ (50.75 Hz) during charging and discharging of the EV. The inverter maintains at least the same power input level of 5.3 kW until $f_{transition}$ (50.75 Hz) is reached during charge. When frequency stepped up from 50 Hz to 50.30 Hz during discharging, the inverter reduces the output power until $f_{transition}$ (50.75 HZ) and discharges − 2.5 kW at 50.30 Hz at 120 s mark in **Figure 12** while the output power of the inverter at 50.20 Hz is − 3.4 kW at 120 s mark as shown in **Figure 28.**

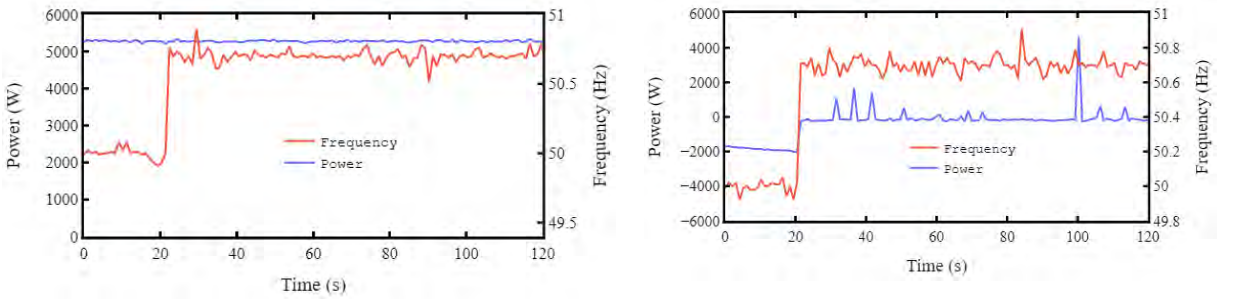


(a) (b)

**Figure 13: Frequency-watt response for step rise in frequency from (50 Hz to 50.70 Hz) (a) charging (b) discharging.**

**Figure 13** shows the frequency-watt response of the inverter for a step rise in frequency from 50 Hz to 50.70 Hz that is between $f_{ULCO}$ (50.25 Hz) and $f_{transition}$ (50.75 Hz) during charging and discharging of the EV. The inverter maintains at least the same power input level of 5.3 kW until $f_{transition}$ (50.75 Hz) is reached during charge. The inverter continues to reduce power output during discharge until $f_{transition}$ (50.75 Hz) is reached and reaches nearly 0 kW at 120 s mark. The inverter reaches lowest power output level in response to increase in $f_{dist}$ between $f_{ULCO}$ and $f_{transition}$ as shown in **Figure 13** (b).

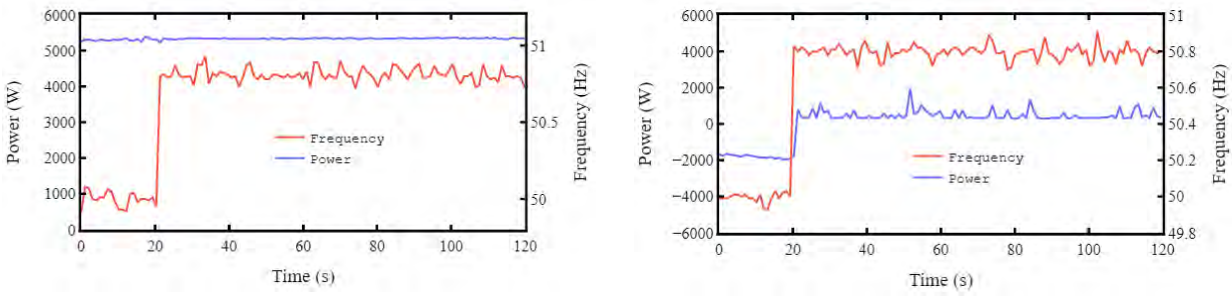


(a) (b)

**Figure 14: Frequency-watt response for step rise in frequency from (50 Hz to 50.80 Hz) (a) charging (b) discharging.**

**Figure 14** shows the frequency-watt response of the inverter for a step rise in frequency from 50 Hz to 50.80 Hz that is just above $f_{transition}$ (50.75 Hz) during charging and discharging of the EV. The frequency-watt response is similar to **Figure 13**.

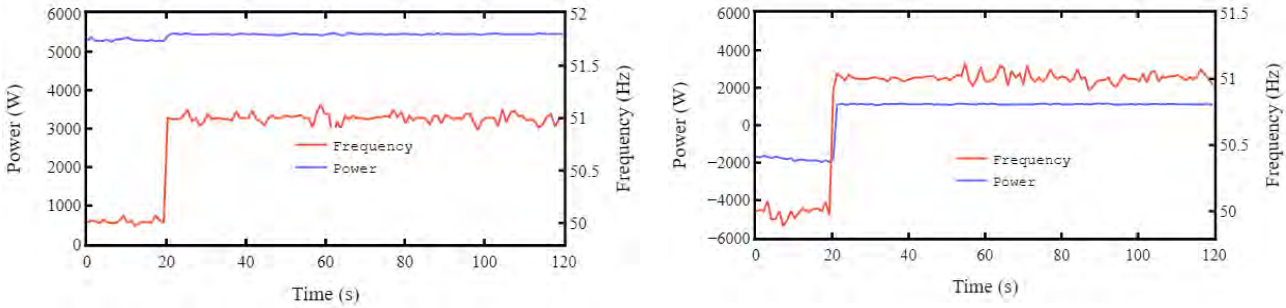


(a) (b)

**Figure 15: Frequency-watt response for step rise in frequency from (50 Hz to 51 Hz) (a) charging (b) discharging.**

**Figure 15** shows the frequency-watt response of the inverter for a step rise in frequency from 50 Hz to 51 Hz that is well above the $f_{transition}$ (50.75 Hz) during charging and discharging of the EV. The inverter increases the power input level linearly with the increase in frequency as shown in **Figure 15**.

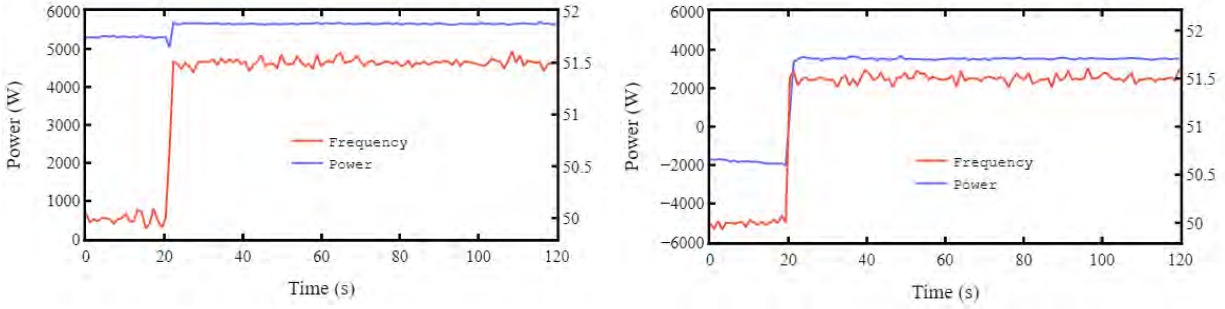


(a) (b)

**Figure 16: Frequency-watt response for step rise in frequency from (50 Hz to 51.5 Hz) (a) charging (b) discharging.**

**Figure 16** shows the frequency-watt response of the inverter for a step rise in frequency from 50 Hz to 51.5 Hz that is well above the $f_{transition}$ (50.75 Hz) during charging and discharging of the EV. Similar behaviour of the inverter is noticed.

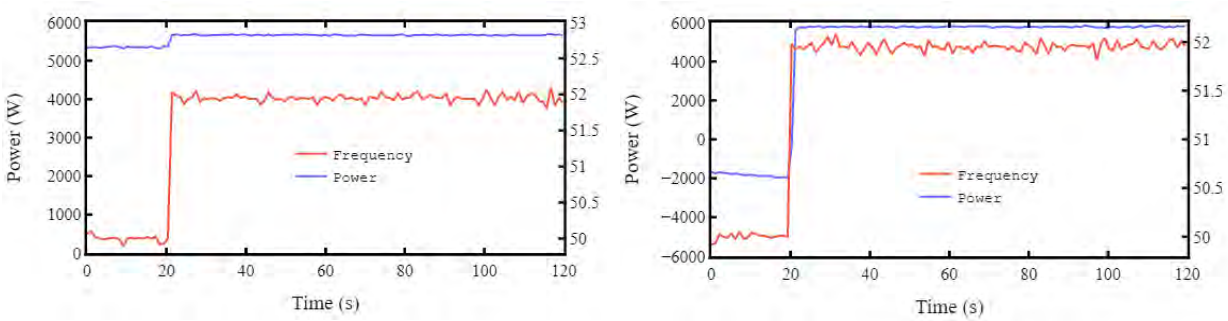


(a) (b)

**Figure 17: Frequency-watt response for step rise in frequency from (50 Hz to 51.95 Hz) (a) charging (b) discharging.**

**Figure 17** shows the frequency-watt response of the inverter for a step rise in frequency from 50 Hz to 51.95 Hz that is between $f_{transition}$ (50.75 Hz) and $f_{Pmin}$ (52 Hz) during charging and discharging of the EV. Similar behaviour of the inverter is noticed. The inverter reaches highest power input level of 5.8 kW in response to increase in frequency between $f_{transition}$ and $f_{Pmin}$ as shown in **Figure 17**.

All the tests results for step rise in frequencies are consistent with AS4777.2:2020.

### C.1.2 Frequency response limits: Step drop in frequency

In this test, an incremental decrease in grid frequencies are created by the grid simulator to verify the frequency-watt response of the inverter in different frequency values from 50 Hz to 47 Hz.

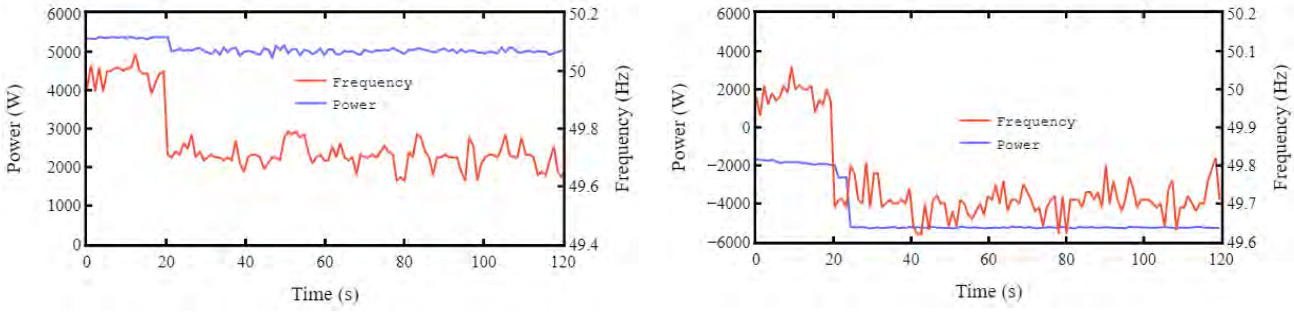


(a) (b)

**Figure 18: Frequency-watt response for step drop in frequency from (50 Hz to 49.70 Hz) (a) charging (b) discharging.**

**Figure 18** shows the frequency-watt response of the inverter for a step drop in frequency from 50 Hz to 49.70 Hz that is below $f_{LLCO}$ during charging and discharging of the EV. The inverter reduces the power input level until $f_{stop-ch}$ (49 Hz) during charge while it maintains at least the same power output level during discharge until $f_{stop-ch}$ (49 Hz) is reached. The output power of the inverter is − 5.2 kW at 120 s mark.

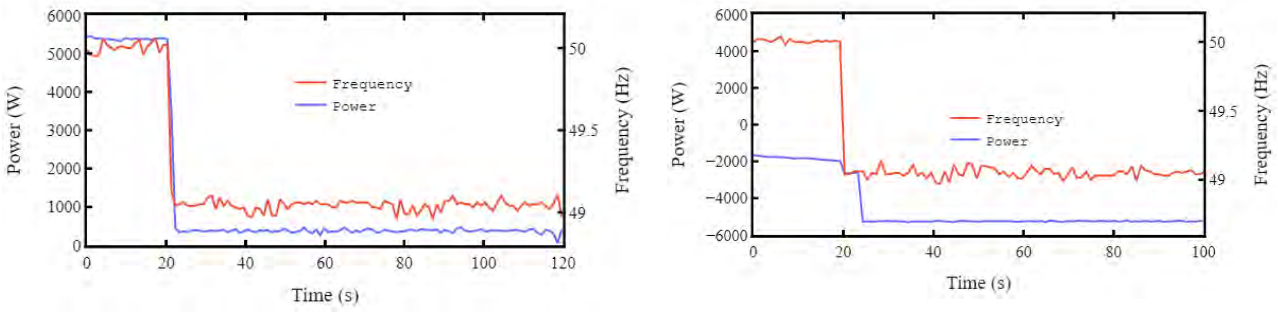


**Figure 19: Frequency-watt response for step drop in frequency from (50 Hz to 49.05 Hz) (a) charging (b) discharging.**

**Figure 19** shows the frequency-watt response of the inverter for a step drop in frequency from 50 Hz to 49.05 Hz that just above the $f_{stop-ch}$ (49 Hz) during charging and discharging of the EV. The inverter continues to reduce the input power level until $f_{stop-ch}$ (49 Hz) drops to 49 Hz during charge. However, the inverter maintains the same output power level during discharge. The output power of the inverter is − 5.2 kW at 100 s mark while the input power reaches close to 0 kW. The inverter reaches this lowest power input level in response to decrease in frequency between $f_{LLCO}$ and $f_{stop-ch}$ as shown in **Figure 19 (a)**.

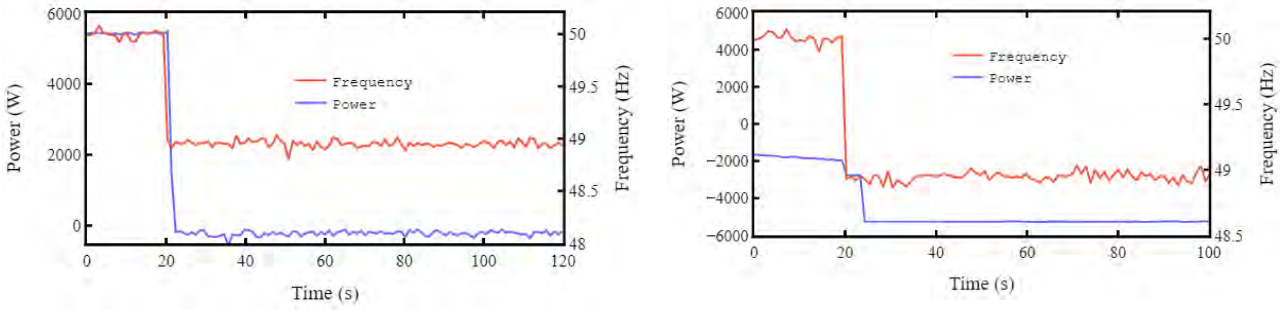


**Figure 20: Frequency-watt response for step drop in frequency from (50 Hz to 48.95 Hz) (a) charging (b) discharging.**

**Figure 20** shows the frequency-watt response of the inverter for a step drop in frequency from 50 Hz to 48.95 Hz that just below the $f_{stop-ch}$ (49 Hz) during charging and discharging of the

EV. The inverter continues to reduce the input power level and ceases charging and starts discharging. However, the inverter maintains the same output power level of − 5.2 kW at 100 s mark during discharge.

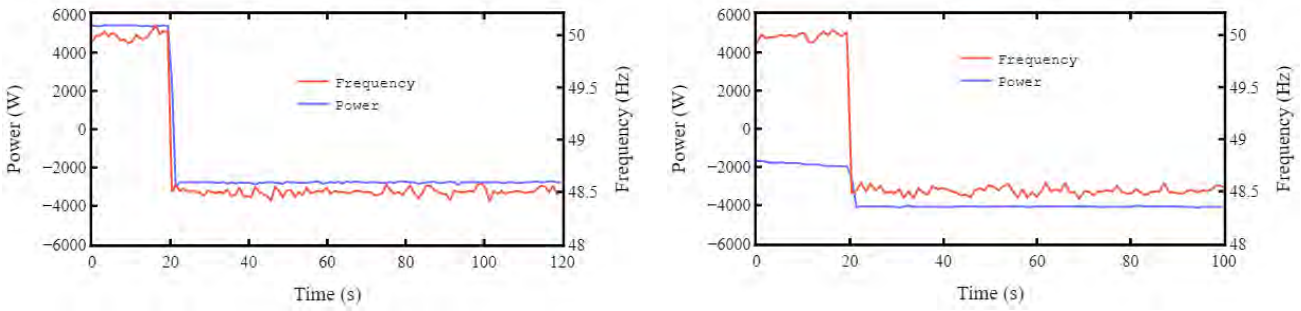


**Figure 21: Frequency-watt response for step drop in frequency from (50 Hz to 48.5 Hz) (a) charging (b) discharging.**

**Figure 21** shows the frequency-watt response of the inverter for a step drop in frequency from 50 Hz to 48.5 Hz that well above the $f_{stop-ch}$ (49 Hz) during charging and discharging of the EV. The inverter increases the power output level linearly with the decrease in frequency.

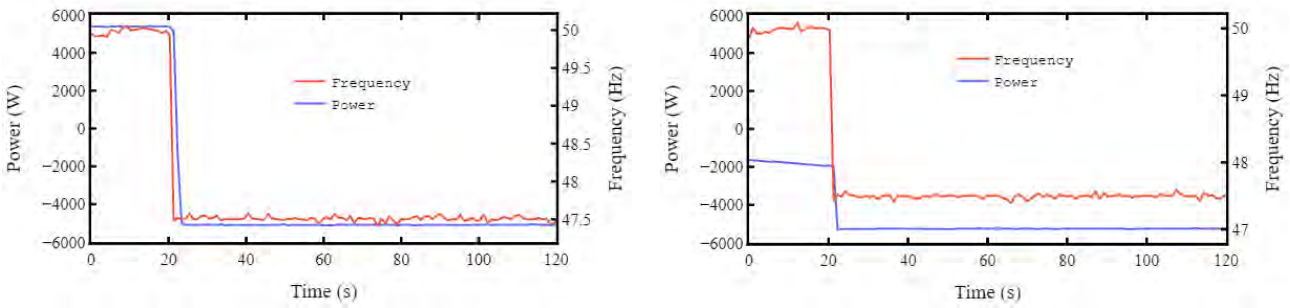


**Figure 22: Frequency-watt response for step drop in frequency from (50 Hz to 47.5 Hz) (a) charging (b) discharging.**

**Figure 22** shows the frequency-watt response of the inverter for a step drop in frequency from 50 Hz to 47.5 Hz that well above the $f_{stop-ch}$ (49 Hz) during charging and discharging of the EV. The inverter response is similar to **Figure 21** and the inverter continues to increase the power output level linearly with the decrease in frequency.

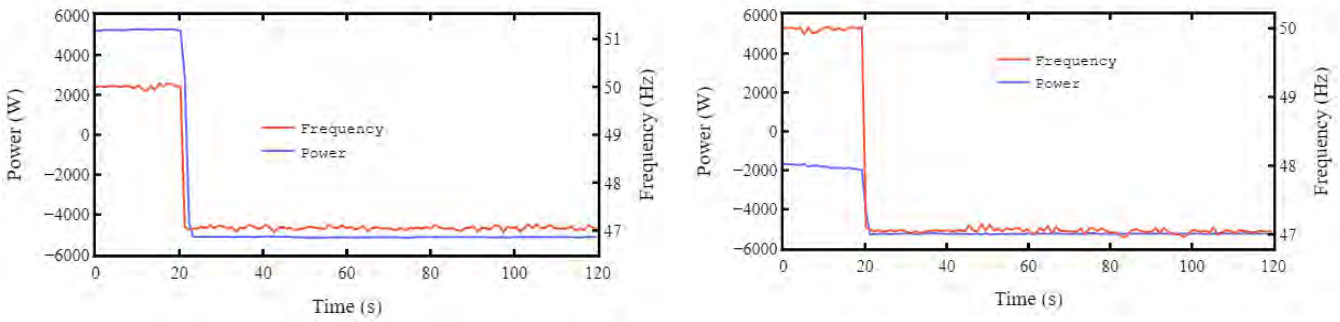


**Figure 23: Frequency-watt response for step drop in frequency from (50 Hz to 47.05 Hz) (a) charging (b) discharging.**

**Figure 23** shows the frequency-watt response of the inverter for a step drop in frequency from 50 Hz to 47.05 Hz that well above the $f_{stop-ch}$ (49 Hz) during charging and discharging of the EV. The inverter continues to increase the power output level linearly with the decrease in frequency until $f_{Pmax}$ (47 Hz) is reached. Also the inverter reaches highest power output level of − 5.4 kW at 120 s mark between $f_{stop-ch}$ and $f_{Pmax}$ as shown in **Figure 23** during discharging.

All the tests results for step drop in frequencies are consistent with AS4777.2:2020.

### C.1.3 Passive anti-islanding frequency limits and frequency notch

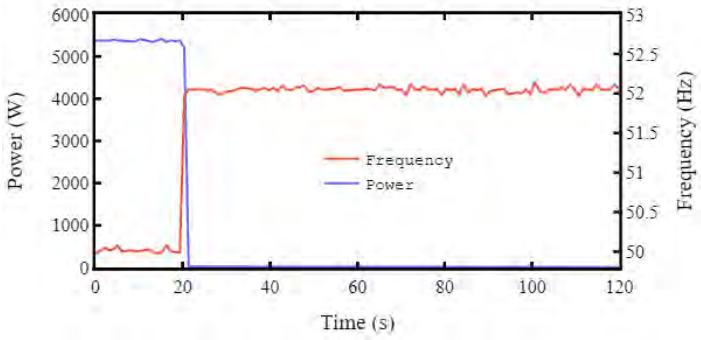


**Figure 24: Frequency step rise during charging (50 Hz to 52.05 Hz).**

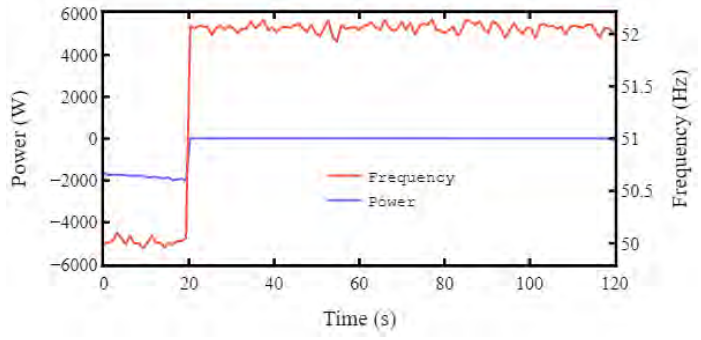

**Figure 25: Frequency step rise during discharging (50 Hz to 52.05 Hz).**

**Figure 24** and **Figure 25** show response of the inverter to a step rise in frequency to 51.95 Hz from 50 Hz during charging and discharging respectively. In both cases, the anti-islanding protective function becomes active and then it disconnects the inverter. The maximum disconnection time is 2 s which is greater than the trip delay time but below the maximum disconnection time.

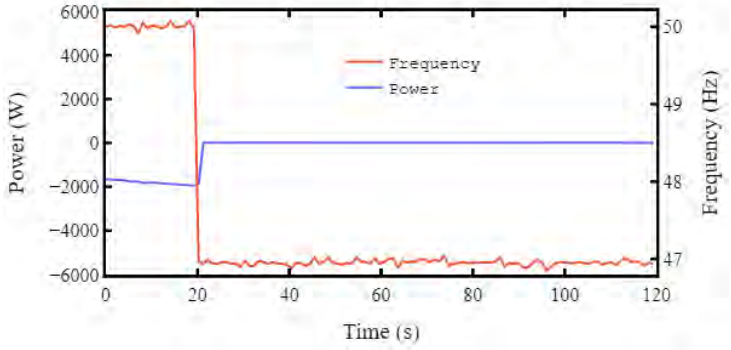


**Figure 26: Frequency step drop during discharging (50 Hz to 46.95 Hz).**

**Figure 26** shows the response of the inverter to a step drop in frequency to 46.95 Hz from 50 Hz during discharging. It is observed that the anti-islanding protective function becomes active and that disconnects the inverter and the maximum disconnection time is 2 s which is greater than the trip delay time but below the maximum disconnection time.

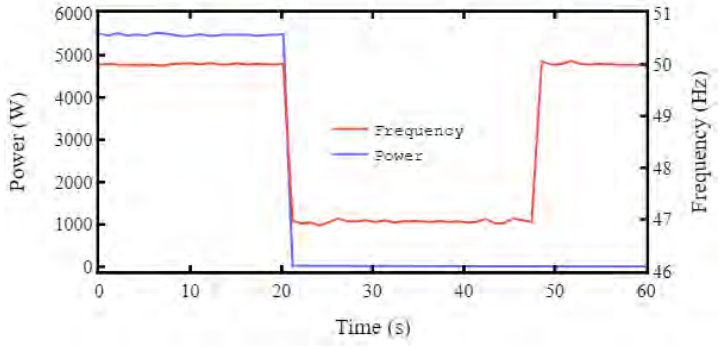


**Figure 27: Frequency notch (50 Hz to 46.95 Hz and then 50Hz) to test anti-islanding protection function.**

**Figure 27** shows the inverter response to a frequency notch from 50 Hz down to 46.95 Hz for 30 s before returning to 50 Hz. The anti-islanding protective function becomes active and then disconnects the inverter at 2 s within the maximum disconnection time. The inverter does not return back to the operation once the frequency returns to 50 Hz.

All the tests results for passive anti-islanding frequency limits are consistent with AS4777.2:2020.

### C.1.4 Frequency variation withstand limit

**Upper limit of continuous operation range, $f_{ULCO}$ (50.25 Hz)**

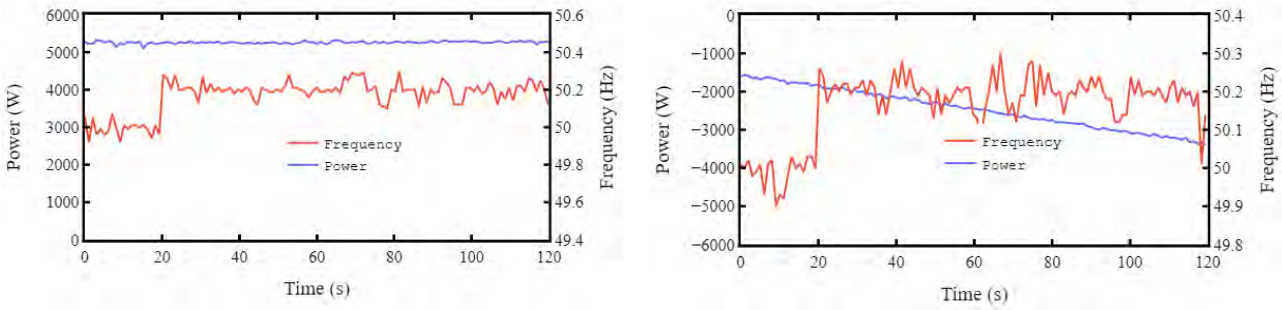


(a) (b)

**Figure 28: Frequency-watt response for step rise in frequency from (50 Hz to 50.20 Hz) (a) charging (b) discharging.**

**Figure 28** shows the frequency-watt response of the inverter for a step rise in frequency which is close to the upper limit of continuous operation ($f_{ULCO}$). The inverter remains in continuous operation and provides continuous charging and discharging power regardless of the step change in frequency as demonstrated in **Figure 28**. This response is consistent with AS4777.2:2020. The charging power is close to 5.3 kW. The discharging power is approximately − 3.4 kW at the 120 s mark and this takes time to ramp up to the rated power which is the limitation of the wallbox firmware at the moment.

**Lower limit of continuous operation range, $f_{LLCO}$ (49.75 Hz)**

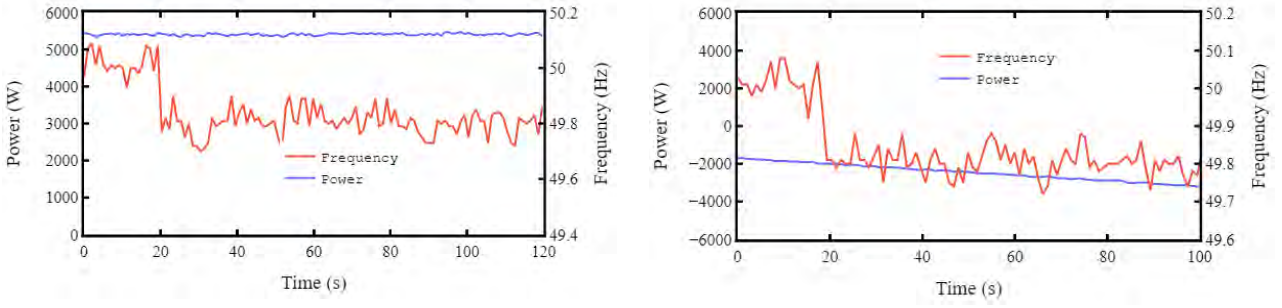


(a) (b)

**Figure 29: Frequency-watt response for step drop in frequency from (50 Hz to 49.8 Hz) (a) charging (b) discharging.**

**Figure 29** shows the frequency-watt response of the inverter for a step drop in frequency which is close to the lower limit of continuous operation ($f_{LLCO}$). The inverter remains in continuous operation and provides continuous charging and discharging power regardless of the step change in frequency as demonstrated in **Figure 29**. This response is consistent with AS4777.2:2020. The charging power is close to 5.5 kW. The discharging power is approximately − 3.5 kW at 100 s mark and this takes time to ramp up to the rated power which is the limitation of the wallbox firmware at the moment.

### C.1.5 RoCoF

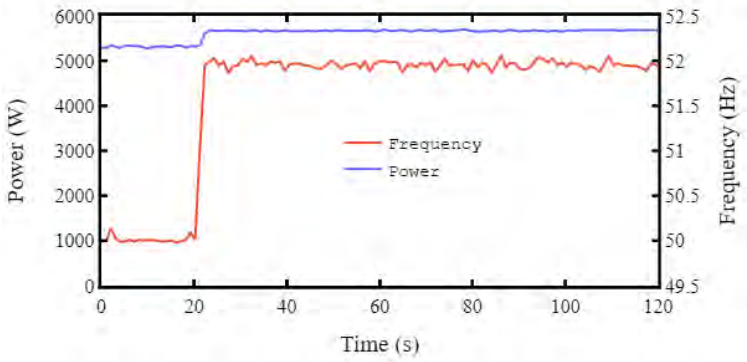


**Figure 30: Inverter power response to 1 Hz/s RoCoF.**

**Figure 30** shows the inverter response to a 1 Hz/s RoCoF disturbance. The inverter can ride through the 1 Hz/s RoCoF disturbance as shown in **Figure 30**. This is desired behaviour of the inverter according to AS4777.2:2020.

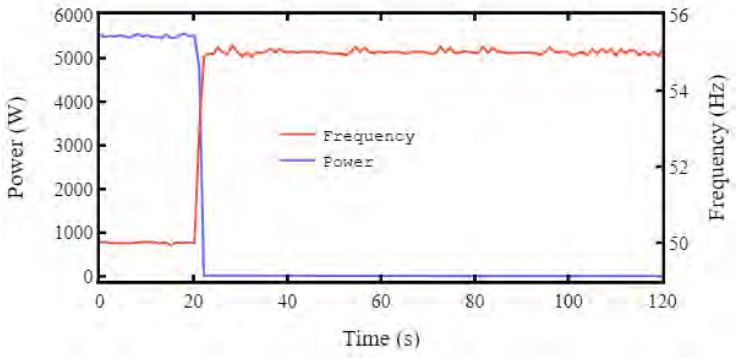


**Figure 31: Inverter power response to 5 Hz/s RoCoF.**

**Figure 31** shows the inverter response to a 5 Hz/s RoCoF disturbance. The inverter does not ride through this disturbance and eventually disconnects at 2 s. This is desired behaviour of the inverter according to AS4777.2:2020.

## C.2 Test results for voltage variables

**Table 33 Voltage standard compliance tests: success criteria**

| Tests | Aim of test | Success criteria |
|---|---|---|
| Under voltage 1<br>Under voltage 2<br>Over voltage 1<br>Over voltage 2 | The aim of the tests is to verify the undervoltage and overvoltage trip delay times and maximum disconnection times of the multiple mode inverter as specified in **Table 27**. | (i) For sustained variation in voltage beyond each limit specified in **Table 27**, the automatic disconnection device shall operate no sooner than the required trip delay time and before the maximum disconnection time.<br>(ii) The inverter shall remain in continuous operation for voltage variations with a duration shorter than the trip delay time as specified in **Table 27**. |
| Voltage limit for sustained operation | The aim of this test is to confirm the over-voltage limit ($V_{norm-max}$) for sustained operation as specified in **Table 28**. | (i) The device should conform to the set-points specified in **Table 28**.<br>(ii) The time to detect a sustained over voltage and disconnect shall be less than 30 s. |
| Voltage disturbance withstanding capability | The aim of this test is to verify the inverter response in accordance with the voltage limits as specified in **Table 29**. | (i) The inverter shall respond as specified in **Table 29** for voltage disturbance.<br>(ii) The inverter shall cease power generation within 200 ms after the measured voltage falls below or exceeds the continuous operation limits as specified in **Table 29**.<br>(iii) For voltage disturbance lasting less than the trip delay times in **Table 27**, the inverter shall restore the power output to the pre-disturbance level within 400 ms after the measured voltage has returned to within the continuous operation limits of **Table 29**. |

### C.2.1 Passive anti-islanding voltage limit

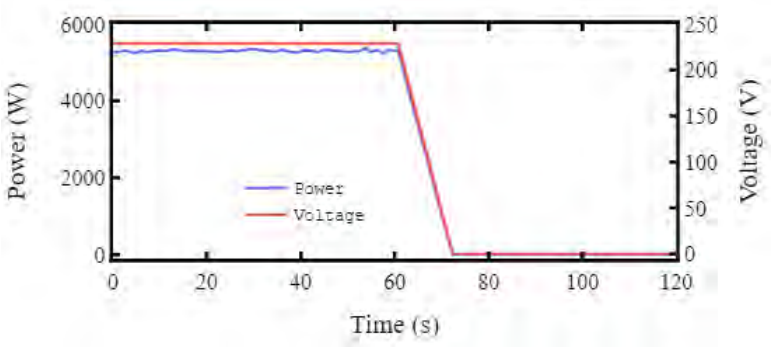


**Figure 32: Inverter power response to under voltage 1 (<180 V).**

An undervoltage 1 disturbance (<180 V) of 160V is applied to the inverter. The inverter sustain the voltage disturbance up to trip delay time (10 s) and disconnects at 11 s which is the maximum disconnection time. The test result is shown in **Figure 32**. This is desired behaviour of the inverter according to AS4777.2:2020.

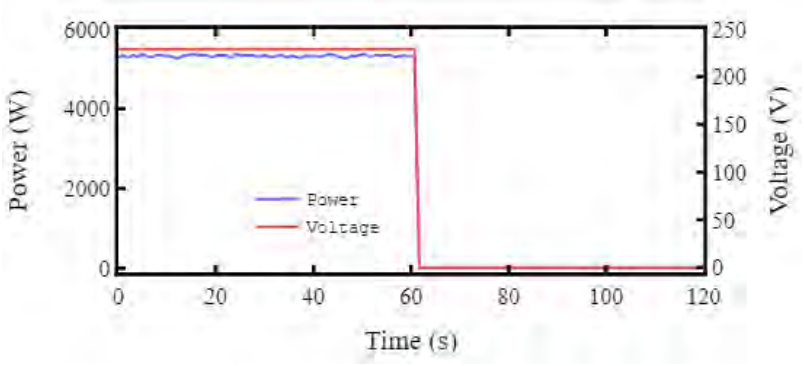


**Figure 33: Inverter power response to under voltage 2 (<70 V).**

An undervoltage 2 disturbance (<70 V) of 65 V is applied to the inverter. The inverter disconnects at 2 s within the maximum disconnection time. The test result is shown **Figure 33**.

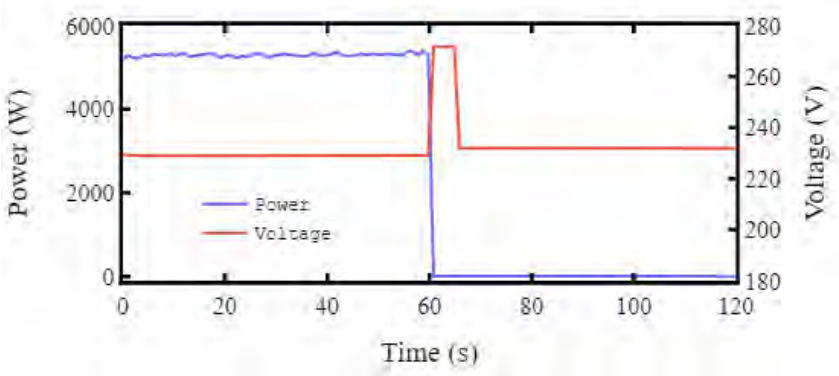


**Figure 34: Inverter power response to over voltage 1 (>265 V).**

An overvoltage 1 disturbance (>265 V) of 270 V is applied to the inverter. It disconnects within 2 s after the overvoltage 1 is applied as shown in **Figure 34**.

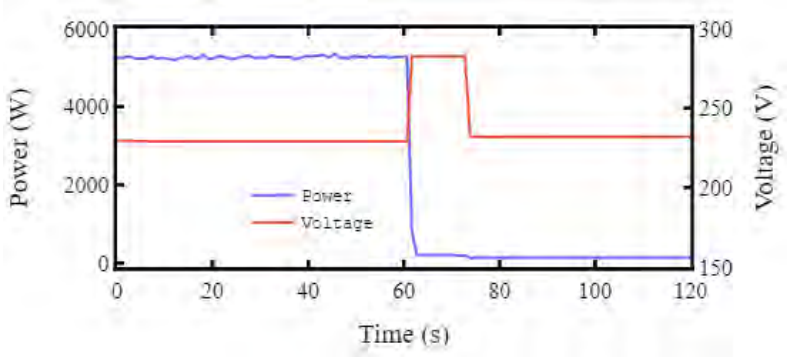


**Figure 35: Inverter power response to over voltage 2 (>275 V).**

An overvoltage 2 disturbance (>275 V) of 282 V is applied to the inverter. It disconnects immediately after the overvoltage 2 disturbance is applied as shown in **Figure 35**.

The test results for passive anti-islanding voltage limits are consistent with AS4777.2:2020 except for the overvoltage 1 test which does not comply with the Australian standard.

### C.2.2 Voltage variation for sustained operation

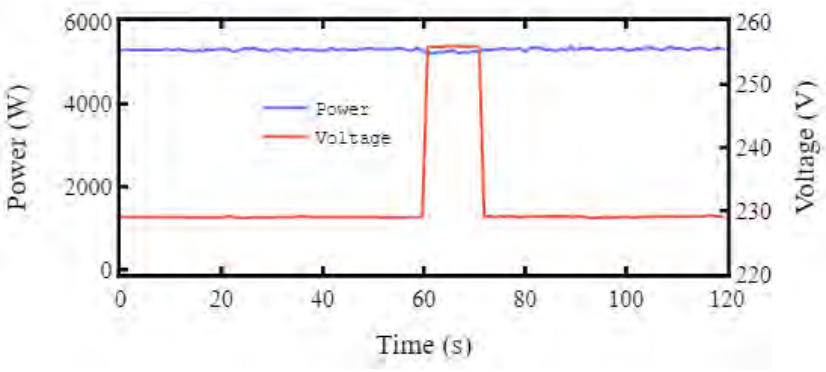


**Figure 36: Inverter power response to $V_{norm-max}$ (=258 V).**

The inverter provides continuous operation up to 258 V as shown in **Figure 36.** The inverter input voltage is stepped up to 258 V from 230 V at 60 s and returned back to 230 V at 72 s. The inverter maintain continuous operation regardless of the step change in input voltage. The test result is consistent with AS4777.2:2020.

### C.2.3 Voltage disturbance response

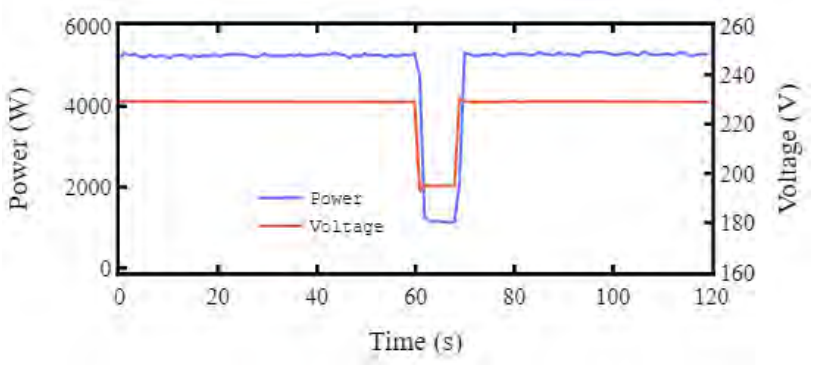


**Figure 37: Inverter power response to a grid voltage between 180 V to 260 V.**

The inverter provides continuous operation 180 V and 260 V as shown in **Figure 37**. There is a sudden drop of voltage from 230 V to 195 V around 60 s for 8 s. The inverter continues operation with reduced the input power during disturbance period and returns back to pre-disturbance level power once the disturbance is cleared.

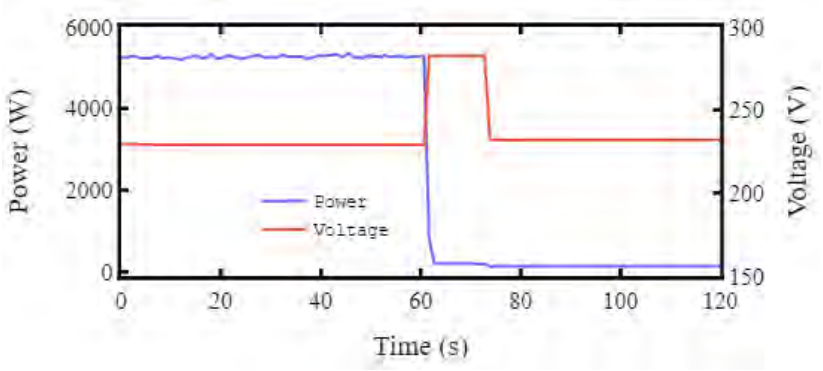


**Figure 38: Inverter power response to a grid voltage (V>260).**

The inverter disconnects from the grid and ceases power generation when the voltage disturbance exceeds 260 V around 60 s as shown in **Figure 38**.

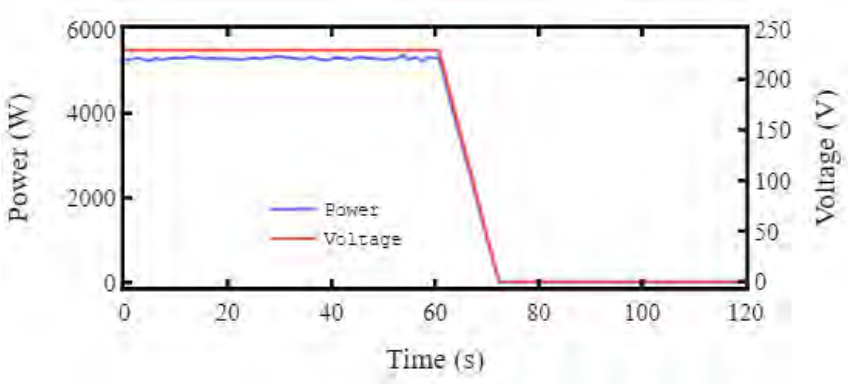


**Figure 39: Inverter power response to a grid voltage (V<180).**

The inverter also ceases power generation when the voltage disturbance falls below 180 V around 61 s as shown in **Figure 39**. The inverter sustain the voltage disturbance up to trip delay time (10 s) and disconnects at 11 s at the maximum disconnection time.

All the tests results for voltage disturbance are consistent with the AS4777.2:2020.

## C.3 Test results for phase angle variables

**Table 34 Phase angle jump variations tests: success criteria**

| Test | Aim of test | Success criteria |
|---|---|---|
| Phase angle jump withstand | The aim of this test is to verify that the inverter complies with the voltage phase angle jump/shift requirement specified in **Table 31**. | (iii) The inverter shall remain in continuous operation for a single phase voltage angle shift within a voltage cycle of at least 60°.<br>(iv) Three phase inverters shall remain in continuous operation for a voltage phase angle shift within a voltage cycle, in the positive sequence, of at least 20°. |

### C.3.1 Phase angle jump withstand requirements

The voltage phase angle has been stepped up with the step change completed within 2 ms and maintained the phase angle for 500 ms (25 cycles). After that, the voltage phase angle has been stepped back to the initial phase angle with the step change completed within 2 ms. **Figure 40** to **Figure 49** represent the initial findings where the inverter can ride through 15°, 20°, 30°, 57°, 60°, 63° degree PAJs but cannot ride through 40°, 45°, 50° and 90° PAJs and gets disconnected from the grid. Therefore, further investigated and testing has been made with 45° degree PAJ in 11 iterations to better understand if the point of occurring PAJ on the voltage waveform has any effect on the riding through behaviour of the inverter. The results are shown through **Figure 50** to **Figure 60**. The test results show that the inverter can ride through the 45° PAJ at few iterations as shown in **Figure 52**, **Figure 56**, and **Figure 58** to **Figure 60**, however it gets disconnected for other iterations. It appears that the point of occurring phase angle jump on voltage waveform has a significant effect on the riding through behaviour. During stepping up the voltage phase angle, the step change in voltage phase angle should occur at the zero crossing of the voltage waveform. During stepping back to the initial phase angle, the step change in phase angle should occur within 45° of the peak or trough of the voltage waveform. The test results are consistent as stipulated in AS4777.2:2020.

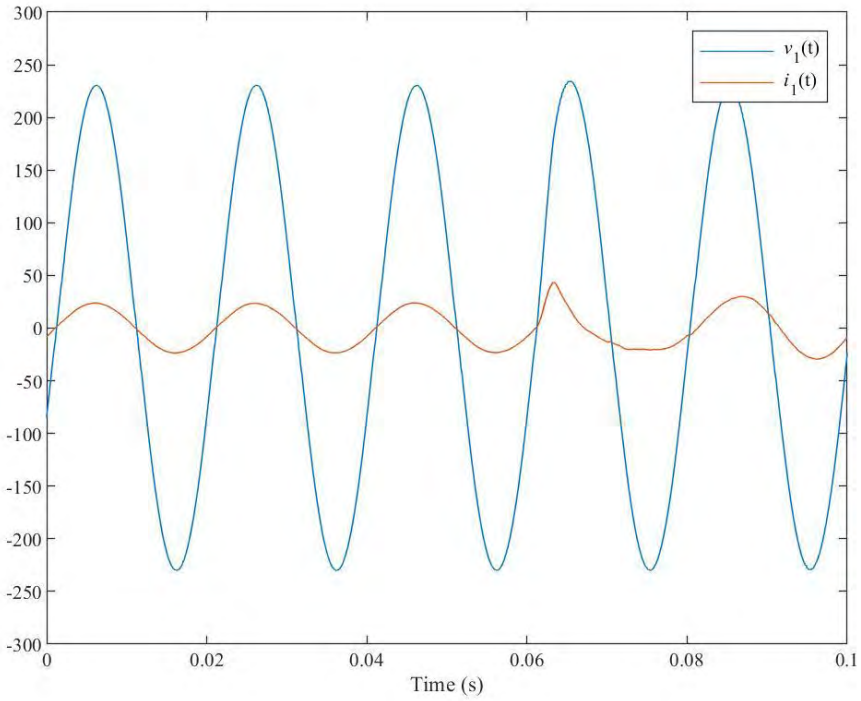


**Figure 40: Inverter response to phase angle jump/shift of 15° (rode through).**

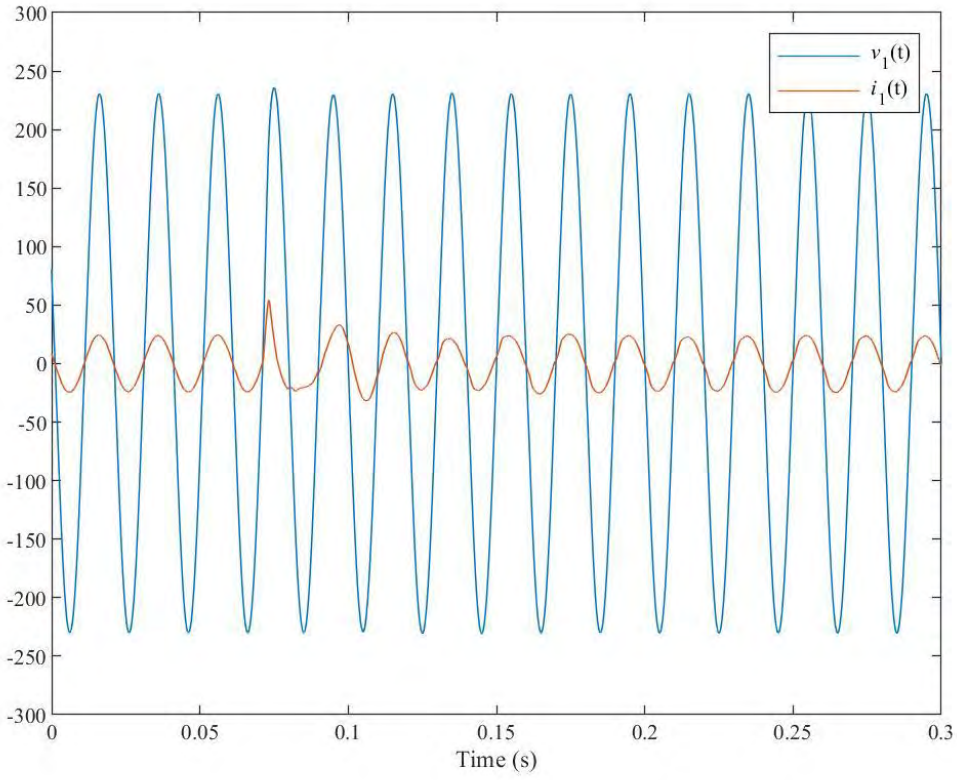


**Figure 41: Inverter response to phase angle jump/shift of 20° (rode through).**

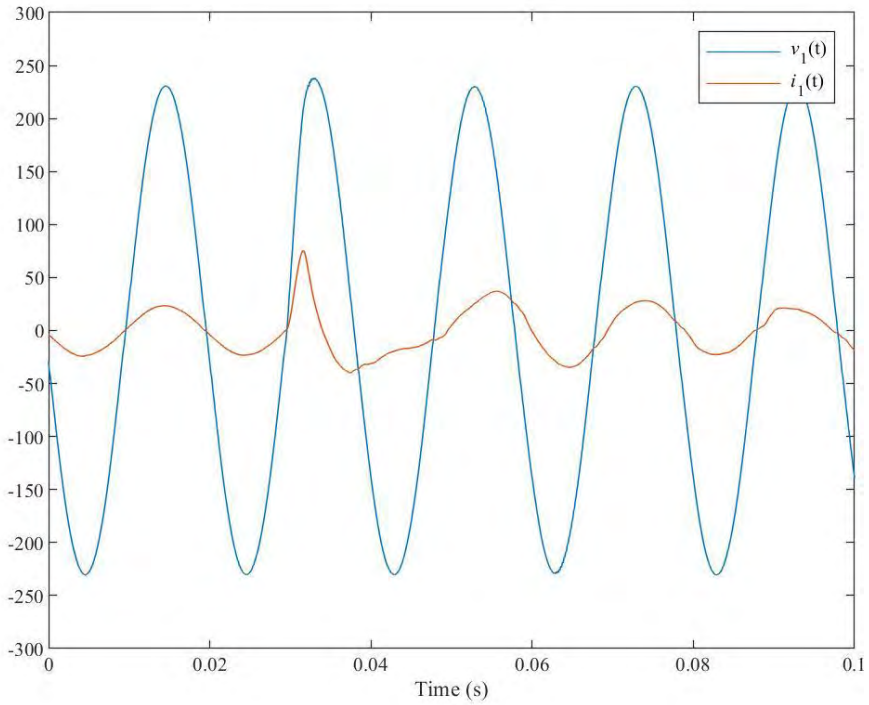


**Figure 42: Inverter response to phase angle jump/shift of 30° (rode through).**

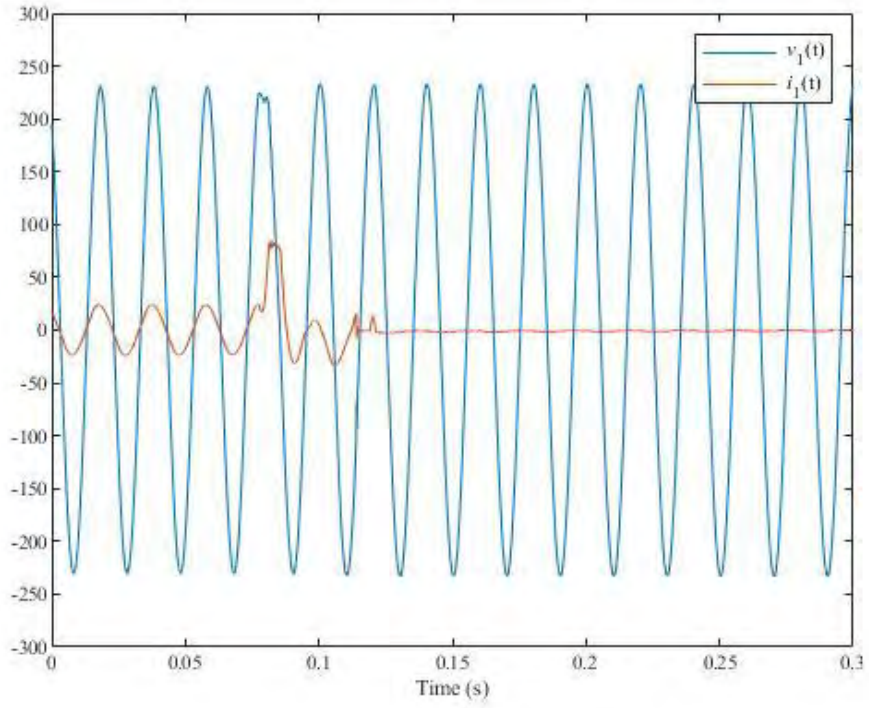


**Figure 43: Inverter response to phase angle jump/shift of 40° (disconnected).**

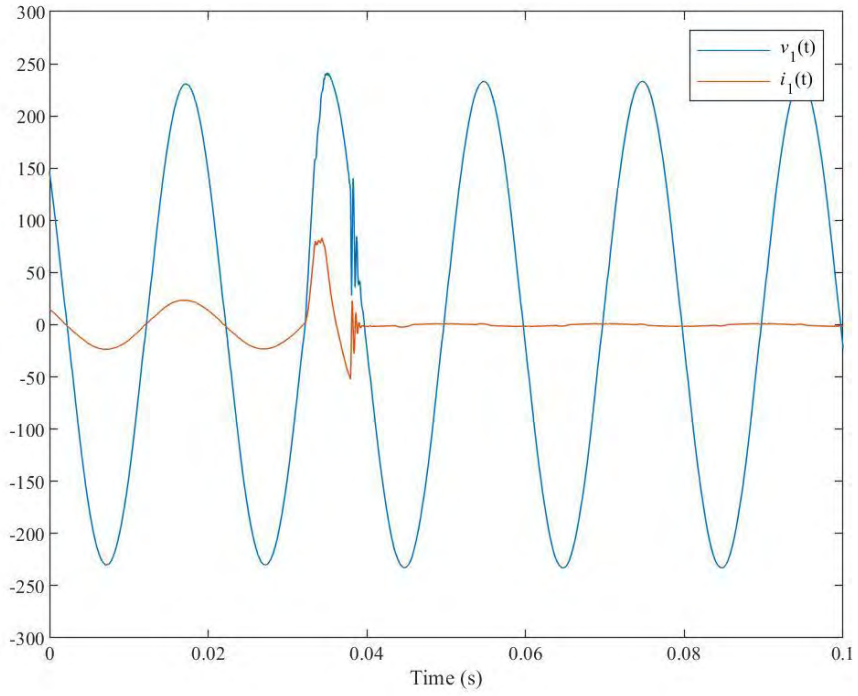


**Figure 44: Inverter response to phase angle jump/shift of 45° (disconnected).**

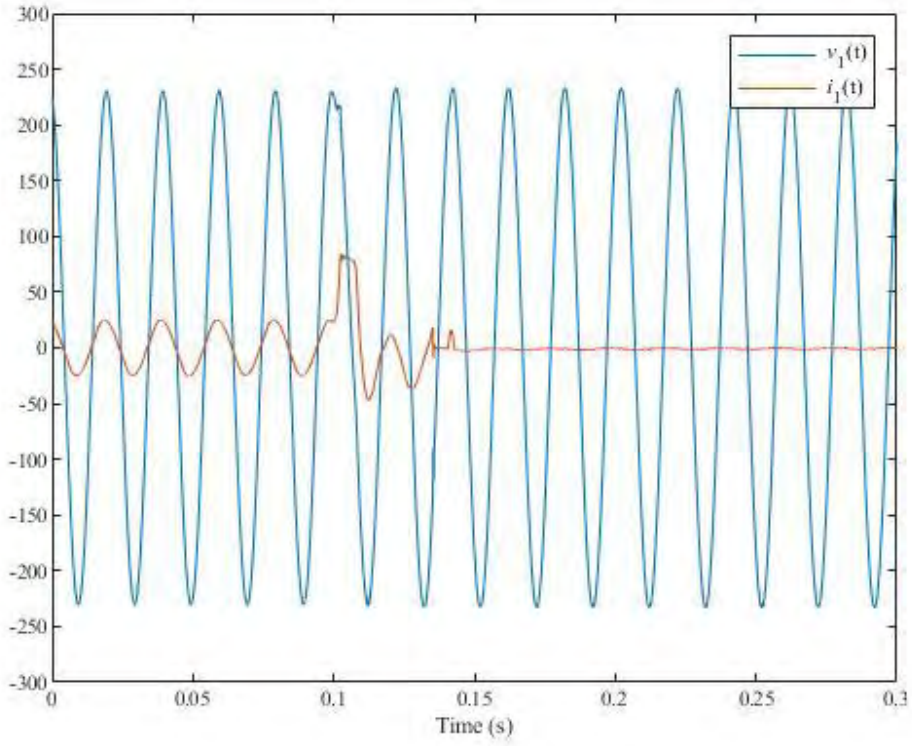


**Figure 45: Inverter response to phase angle jump/shift of 50° (disconnected).**

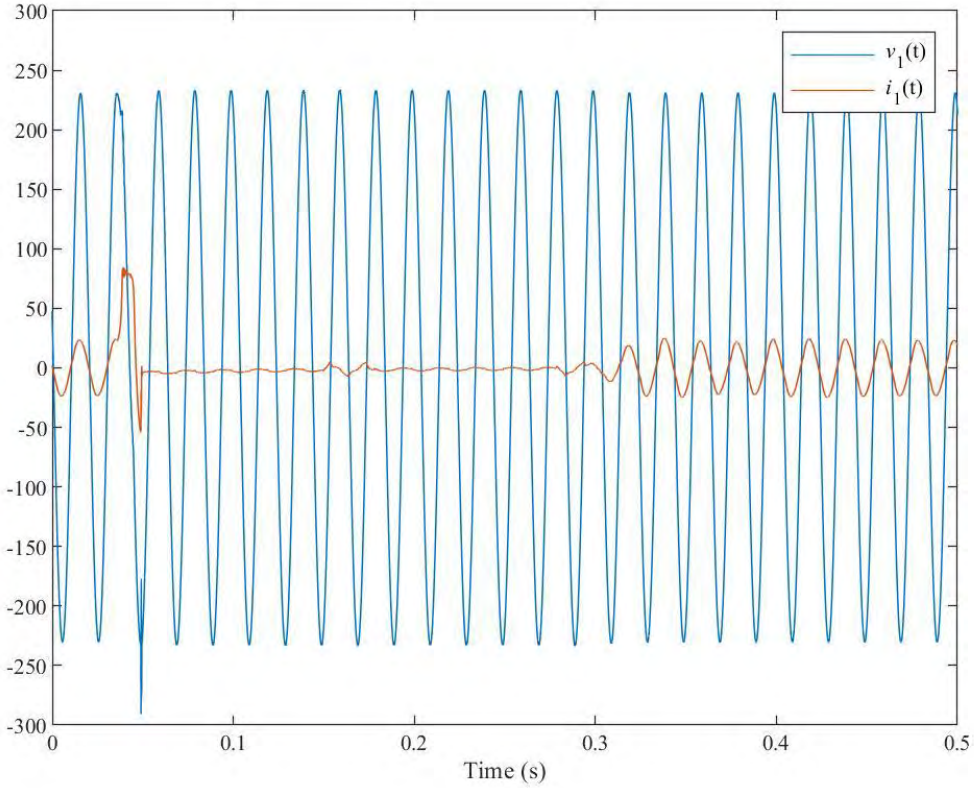


**Figure 46: Inverter response to phase angle jump/shift of 57° (rode through).**

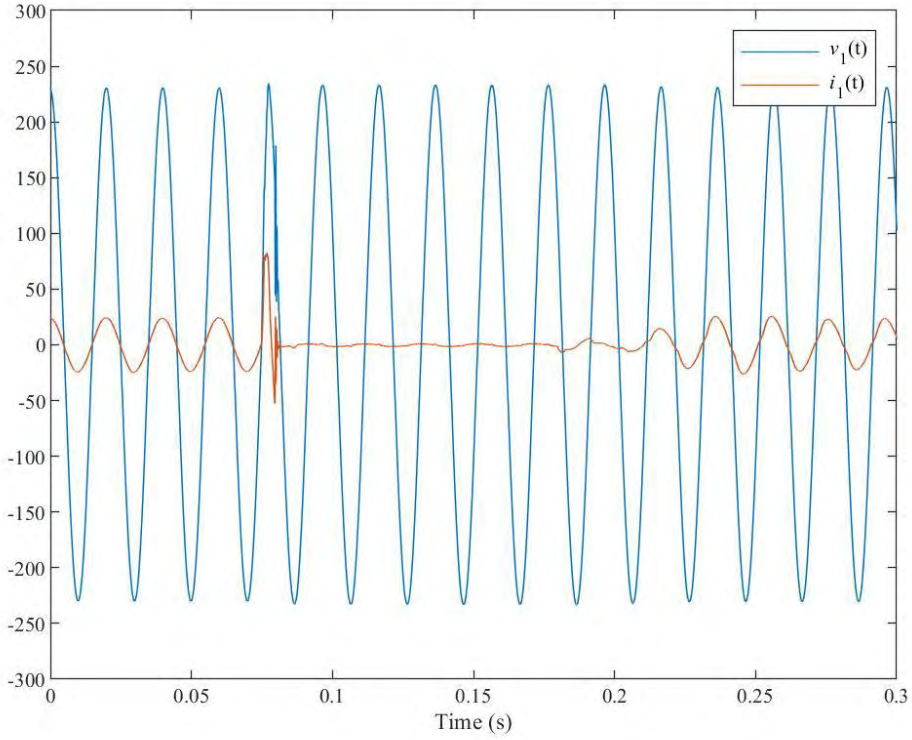


**Figure 47: Inverter response to phase angle jump/shift of 60° (rode through).**

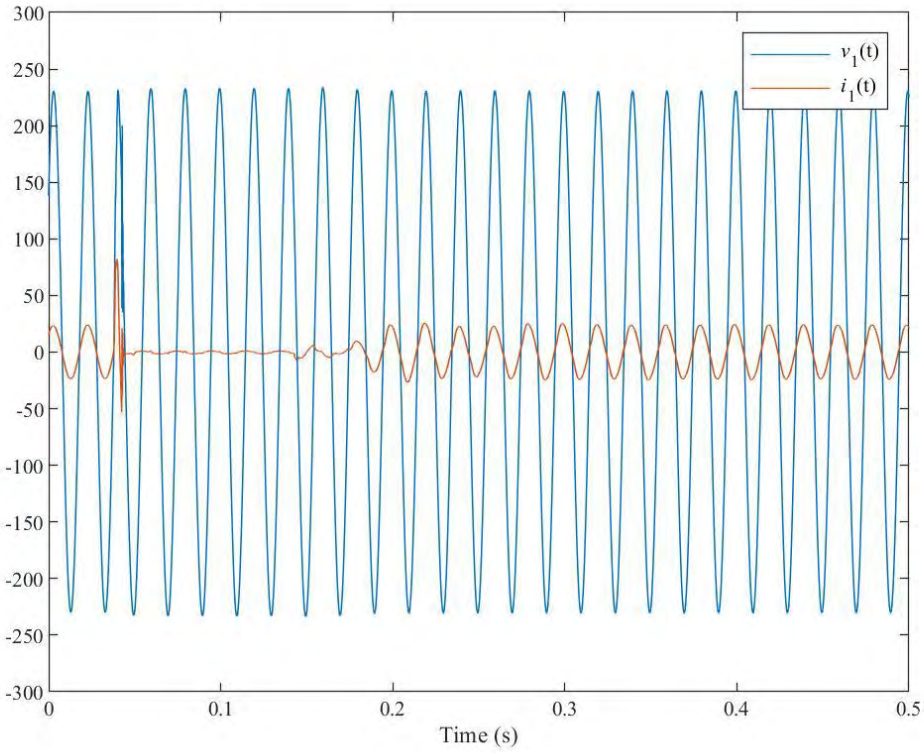


**Figure 48: Inverter response to phase angle jump/shift of 63° (rode through).**

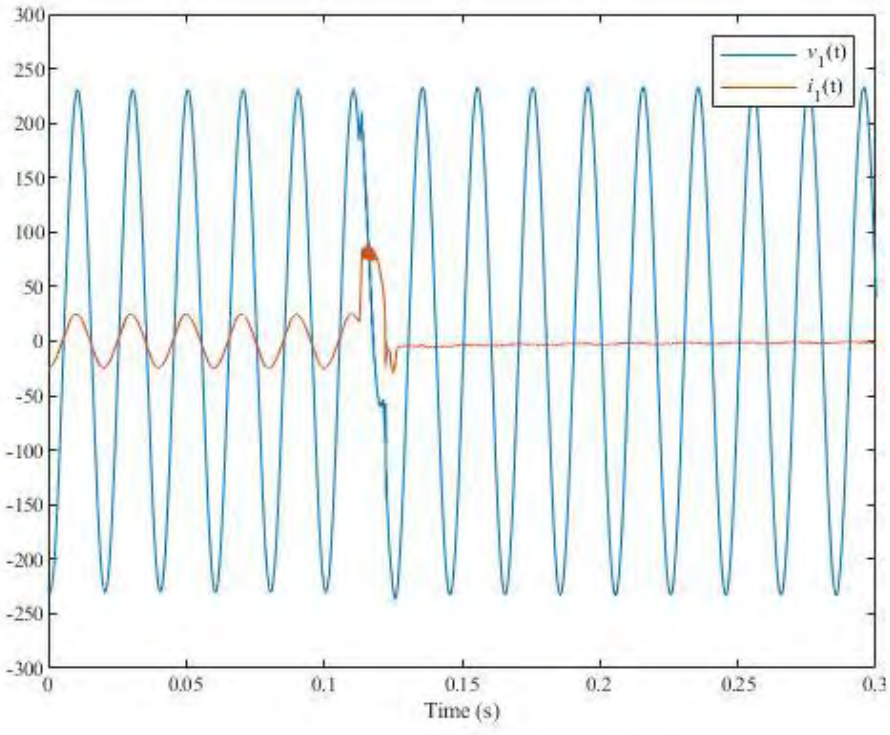


**Figure 49: Inverter response to phase angle jump/shift of 90° (disconnected).**

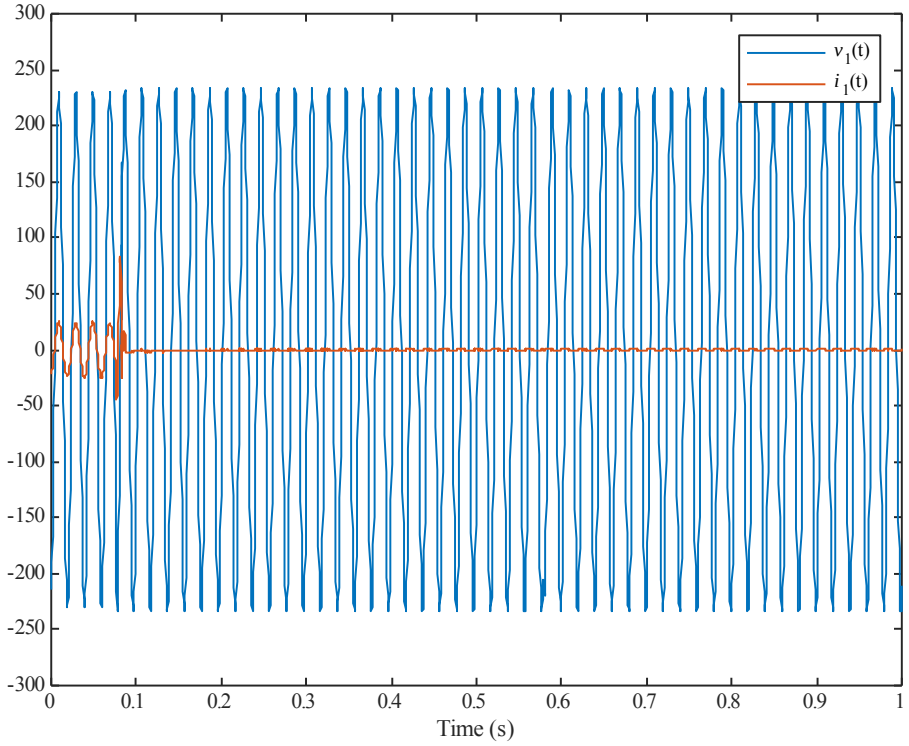


(a)

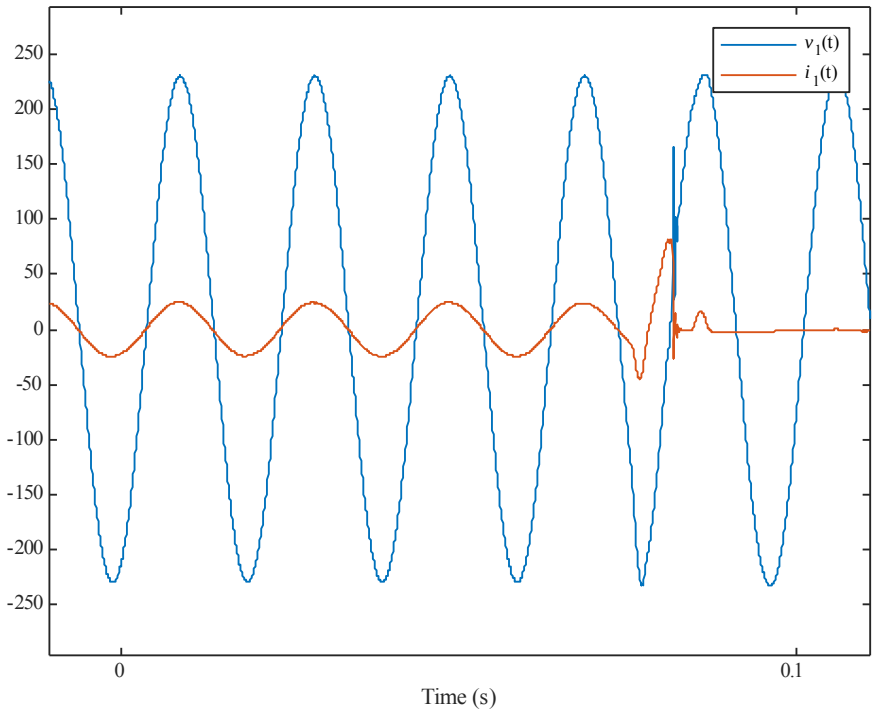


(b)

**Figure 50: Inverter response to phase angle jump/shift of 45° - iteration 1, (disconnected).**

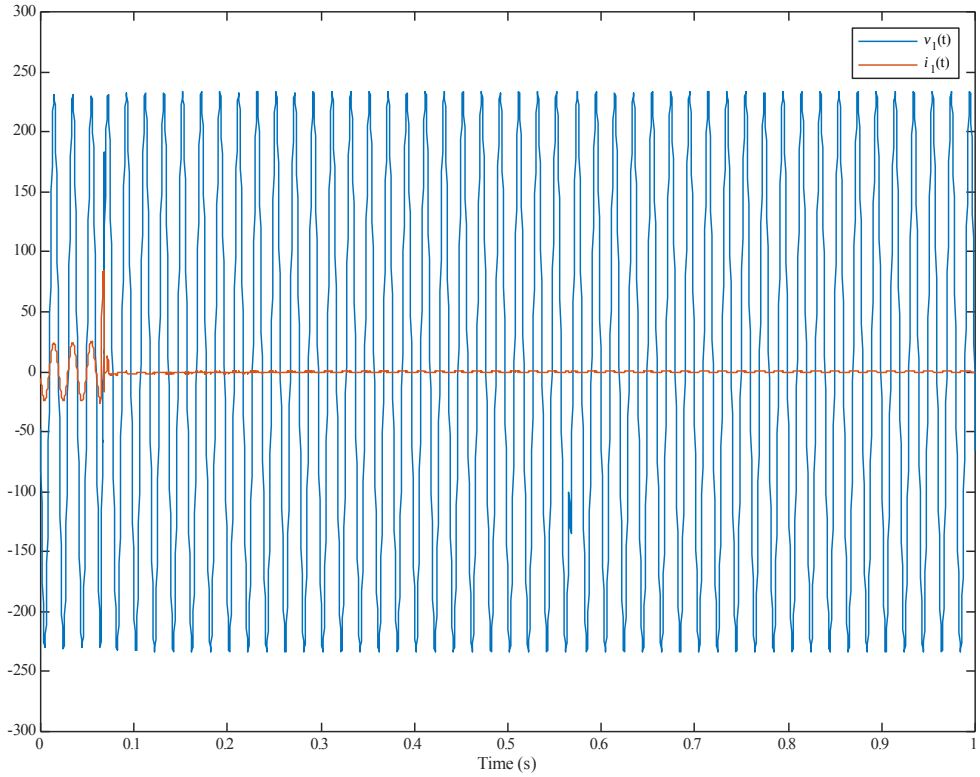


(a)

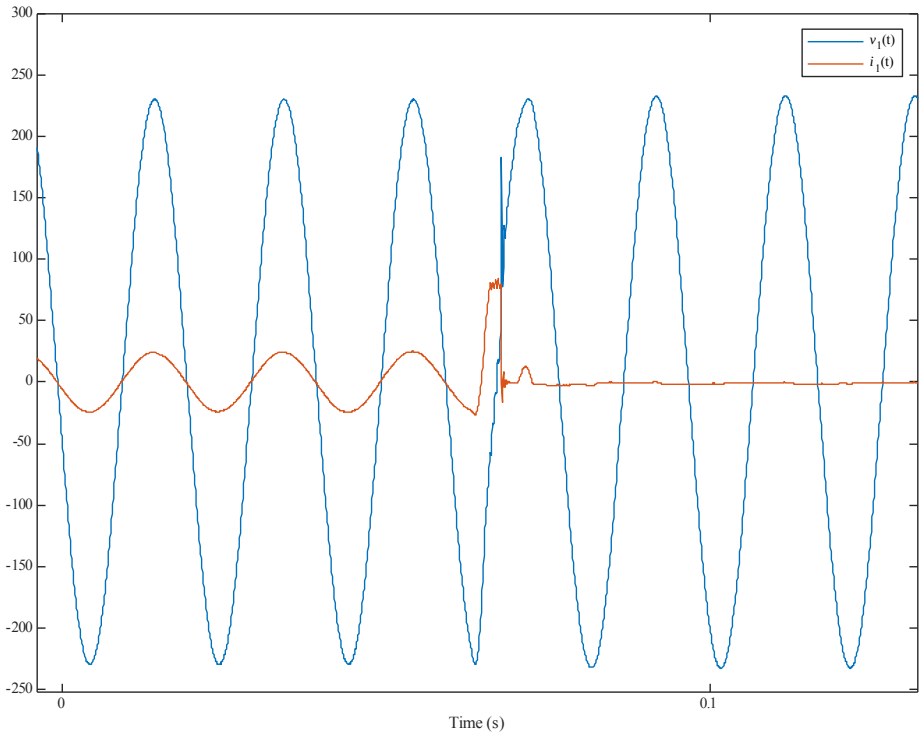


(b)

**Figure 51: Inverter response to phase angle jump/shift of 45° - iteration 2, (disconnected).**

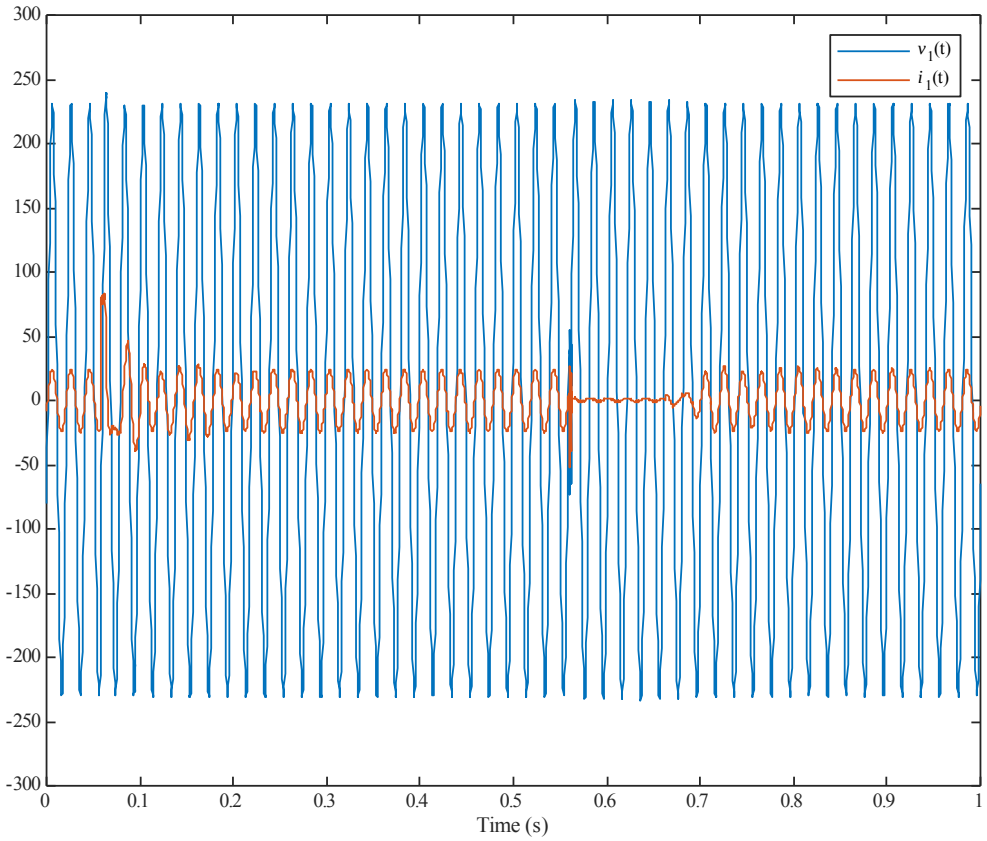
$v_1(t)$
$i_1(t)$
300
250
200
150
100
50
0
-50
-100
-150
-200
-250
-300
0
0.1
0.2
0.3
0.4
0.5
0.6
0.7
0.8
0.9
1
Time (s)

(a)

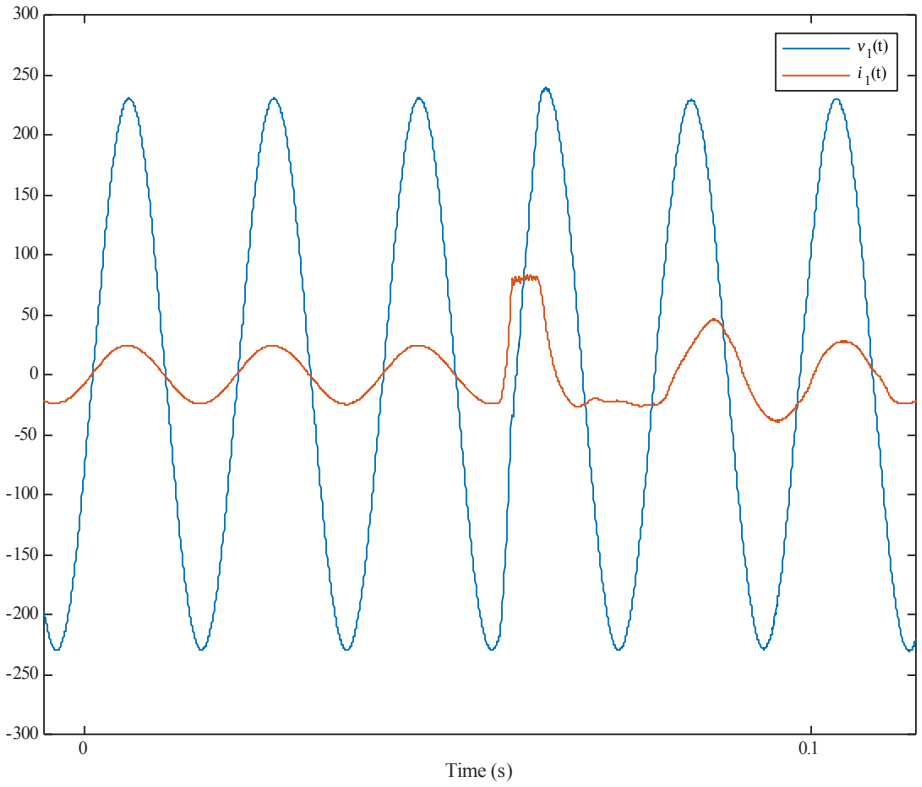
$v_1(t)$
$i_1(t)$
300
250
200
150
100
50
0
-50
-100
-150
-200
-250
-300
0
0.1
Time (s)

(b)

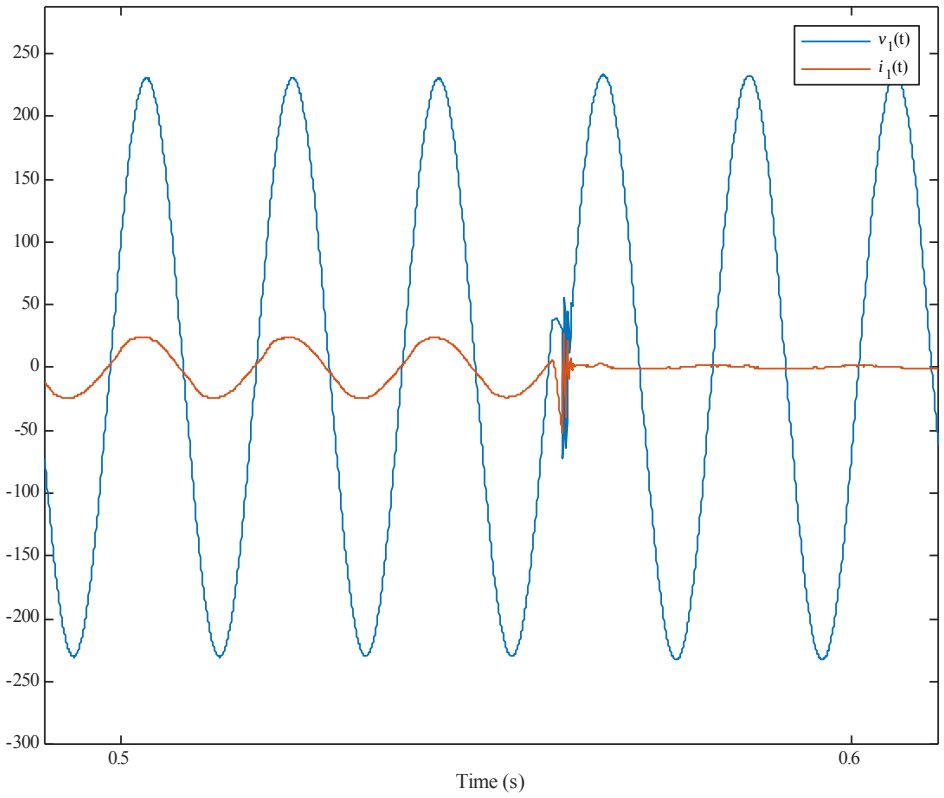


(c)

**Figure 52: Inverter response to phase angle jump/shift of 45° - iteration 3, (rode through).**

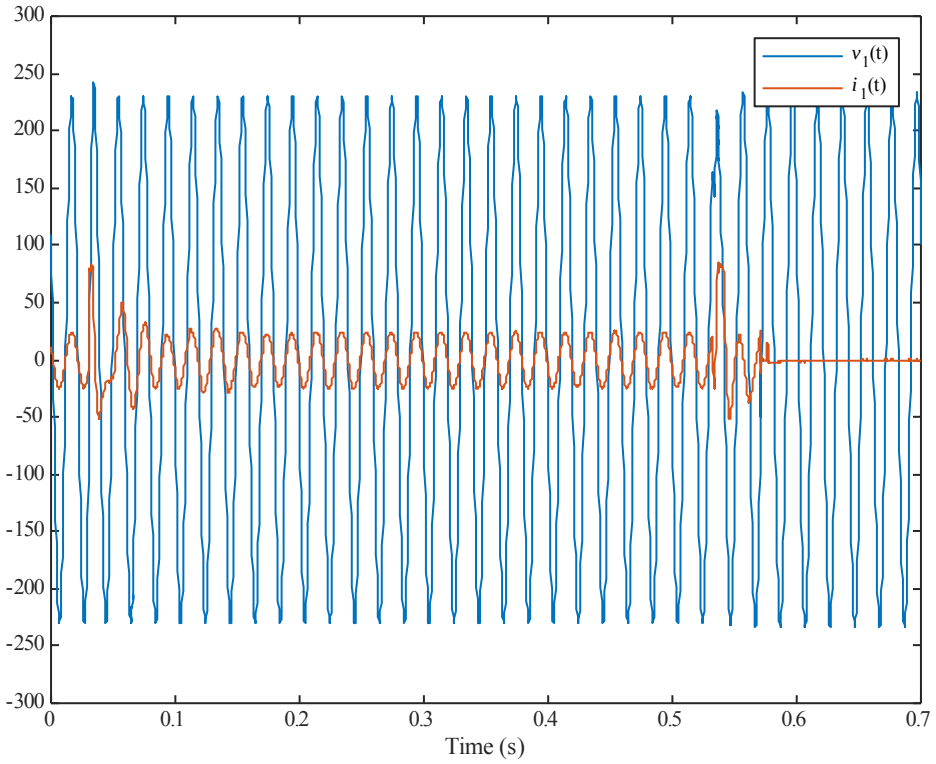


(a)

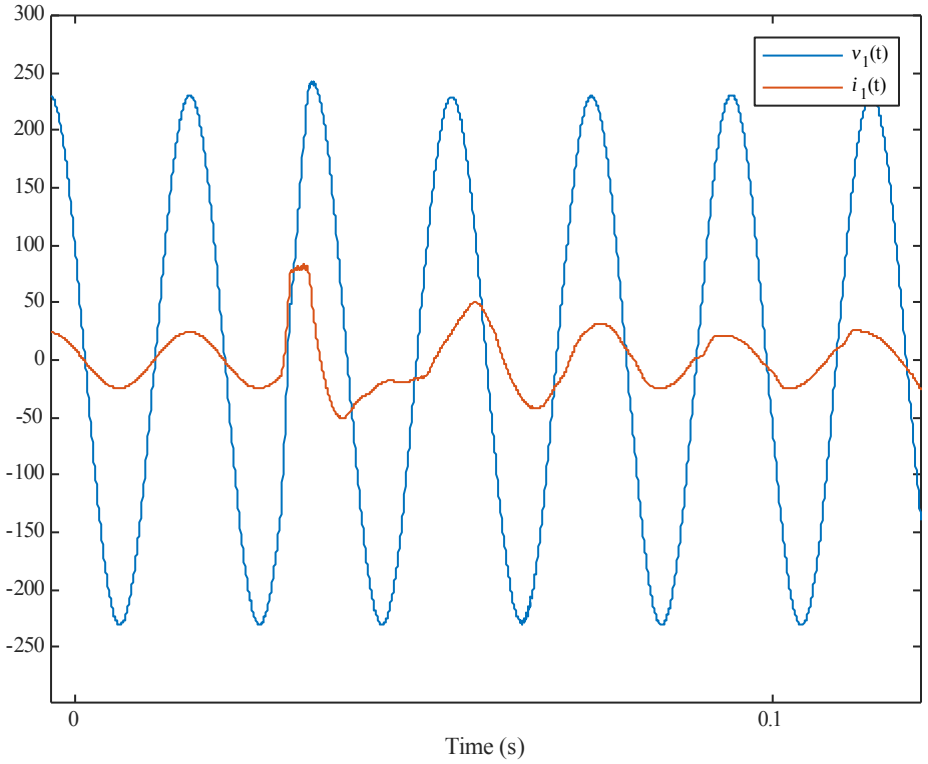


(b)

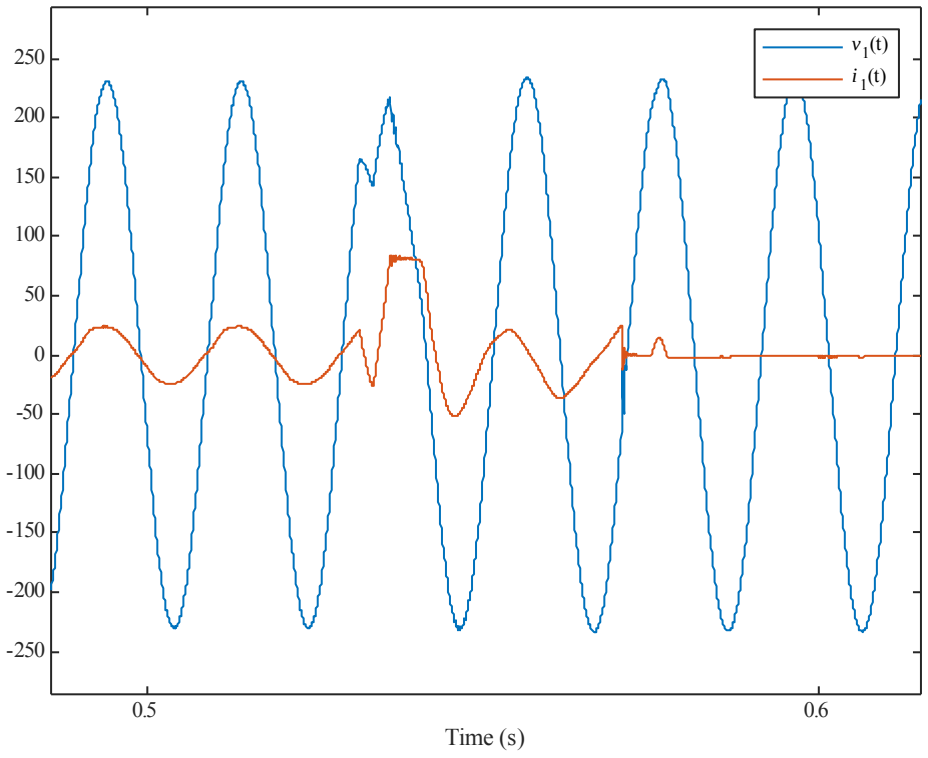


(c)

**Figure 53: Inverter response to phase angle jump/shift of 45° - iteration 4, (disconnected).**

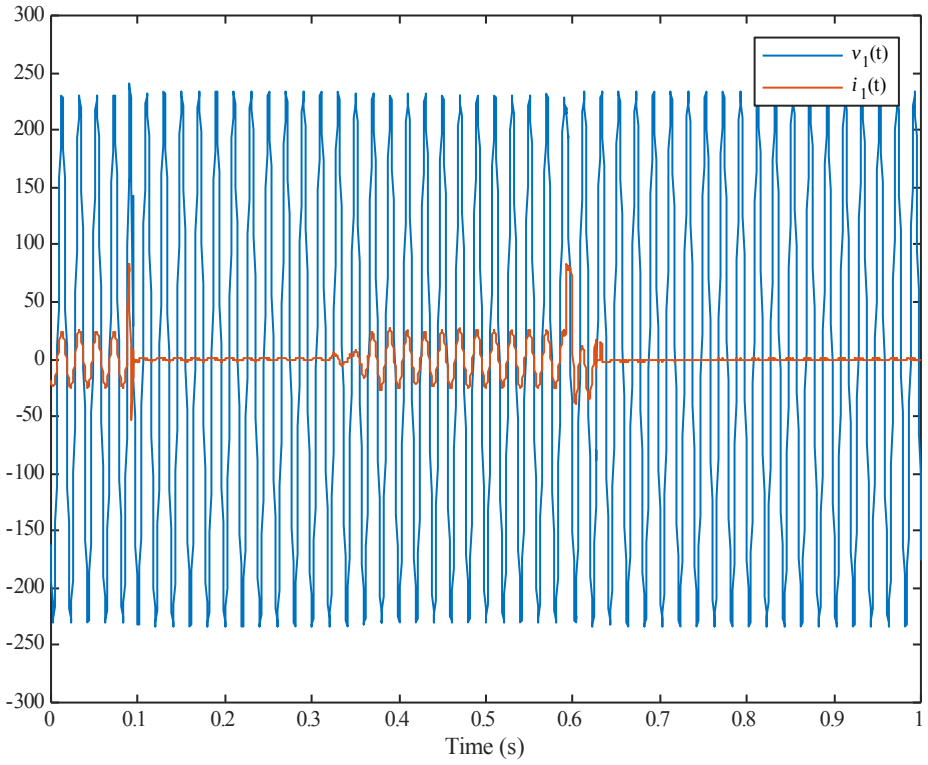
300
250
200
150
100
50
0
-50
-100
-150
-200
-250
-300
0
0.1
0.2
0.3
0.4
0.5
0.6
0.7
0.8
0.9
1
Time (s)
$v_1(t)$
$i_1(t)$

(a)

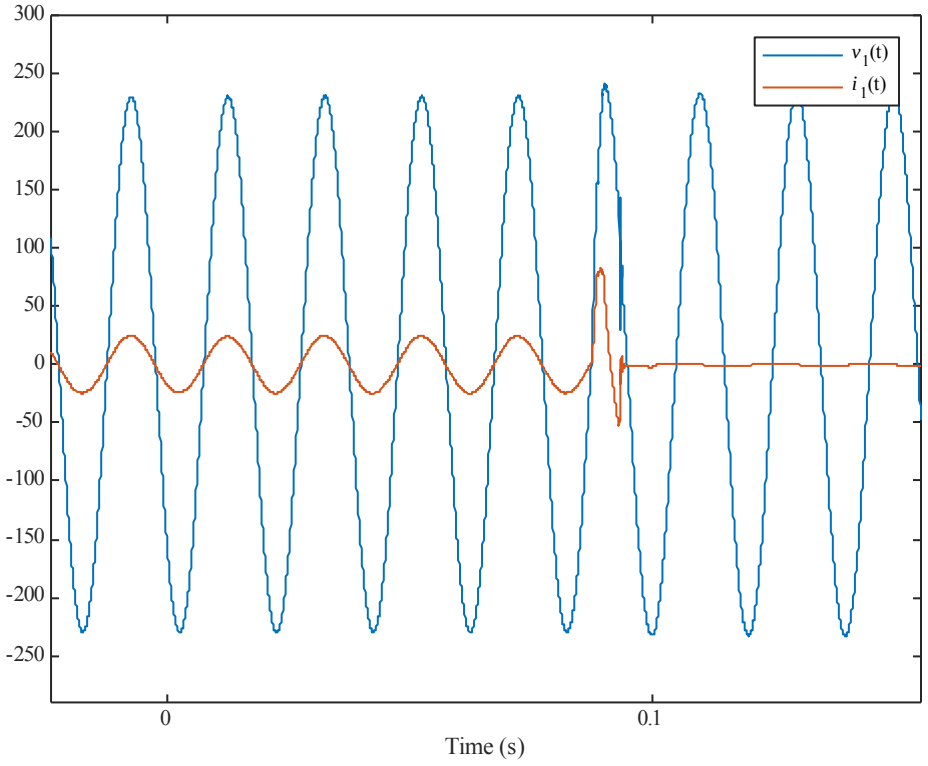
300
250
200
150
100
50
0
-50
-100
-150
-200
-250
0
0.1
Time (s)
$v_1(t)$
$i_1(t)$

(b)

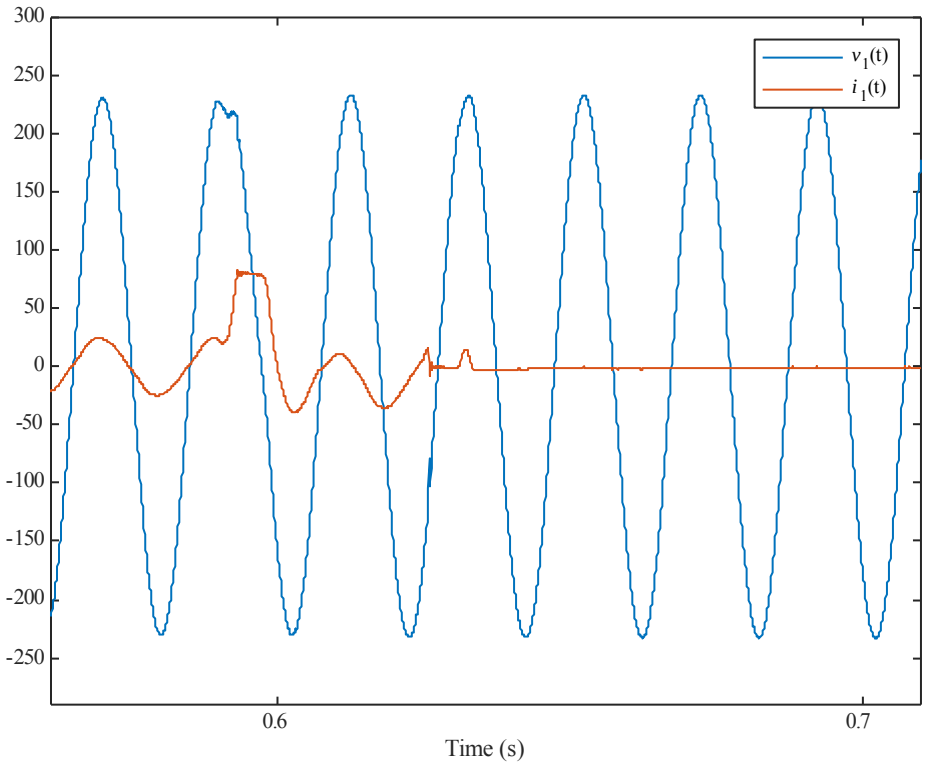


(c)

**Figure 54: Inverter response to phase angle jump/shift of 45° - iteration 5, (disconnected).**

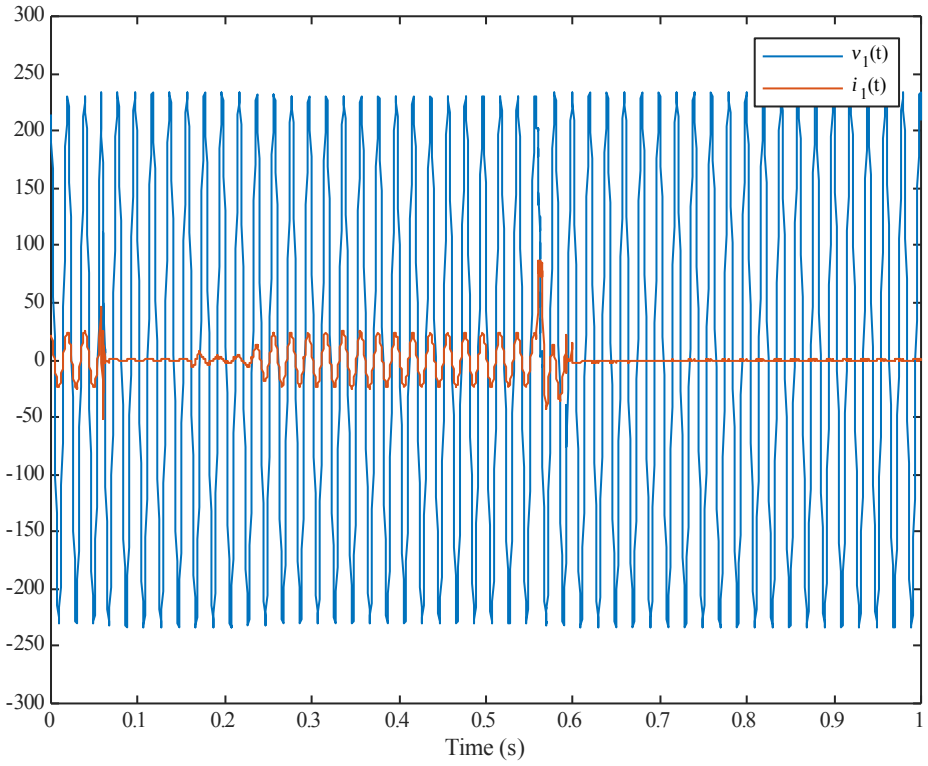


(a)

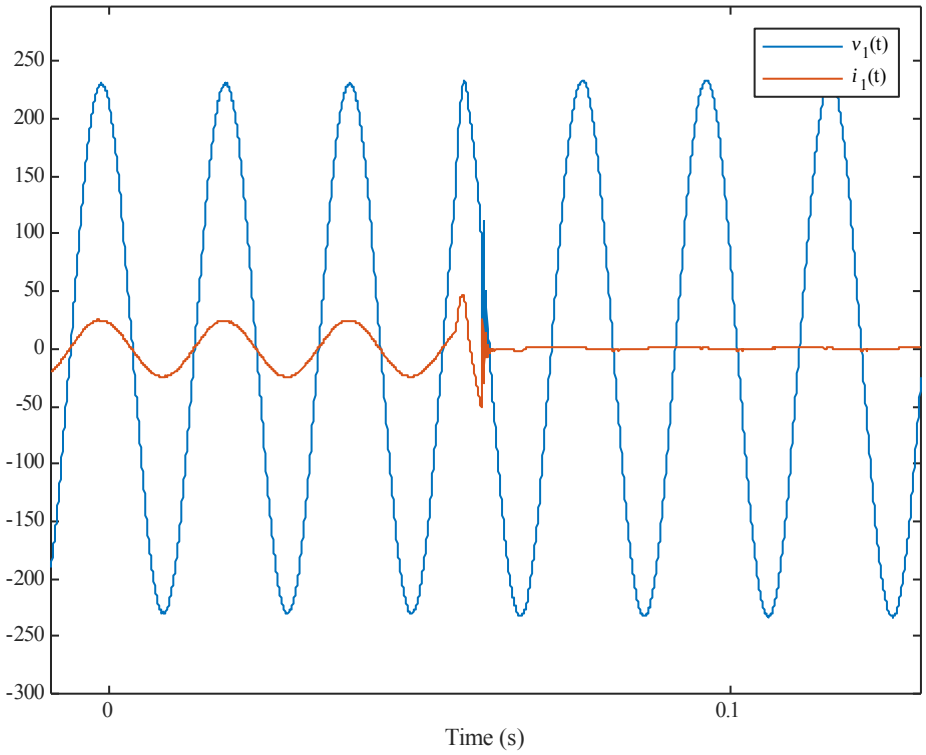


(b)

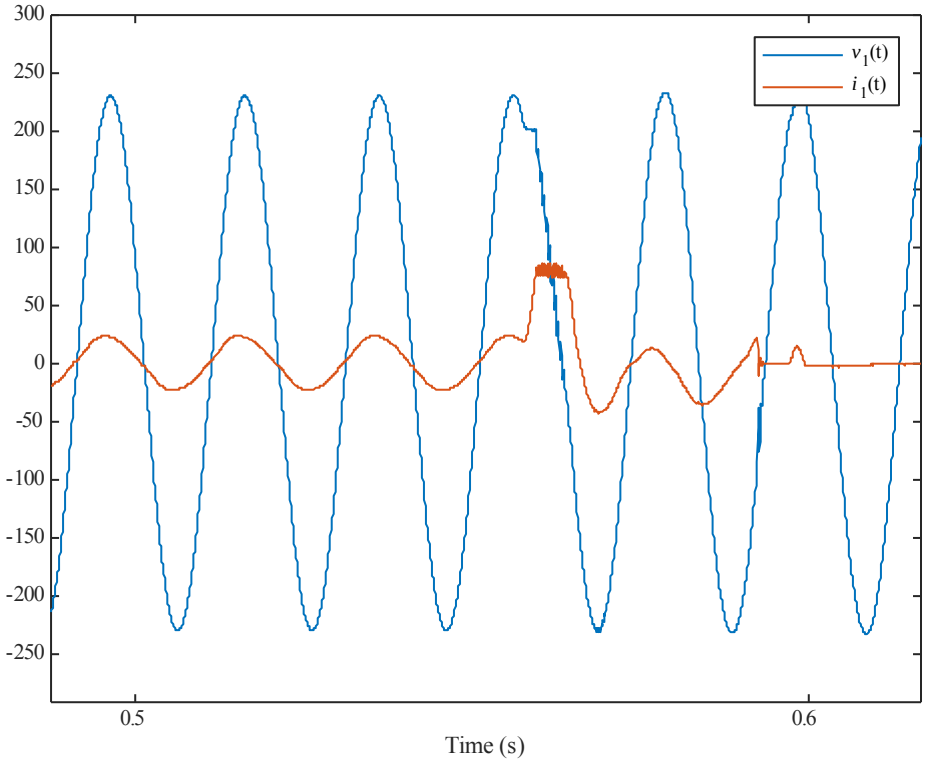


(c)

**Figure 55: Inverter response to phase angle jump/shift of 45° - iteration 6, (disconnected).**

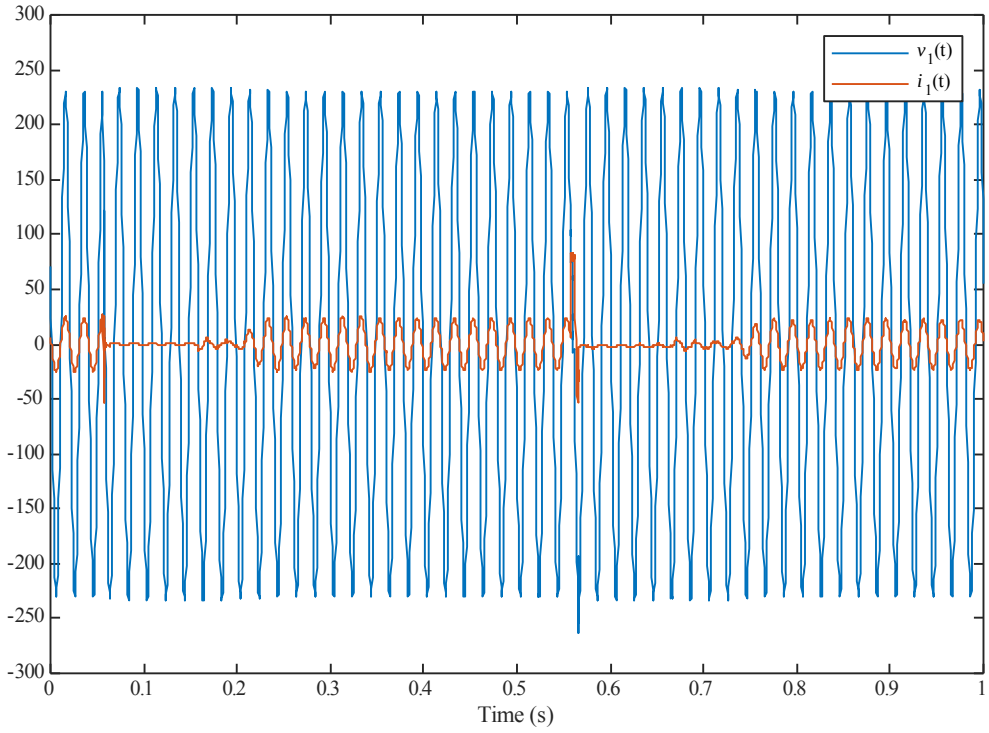
$v_1(t)$
$i_1(t)$
300
250
200
150
100
50
0
-50
-100
-150
-200
-250
-300
0
0.1
0.2
0.3
0.4
0.5
0.6
0.7
0.8
0.9
1
Time (s)

(a)

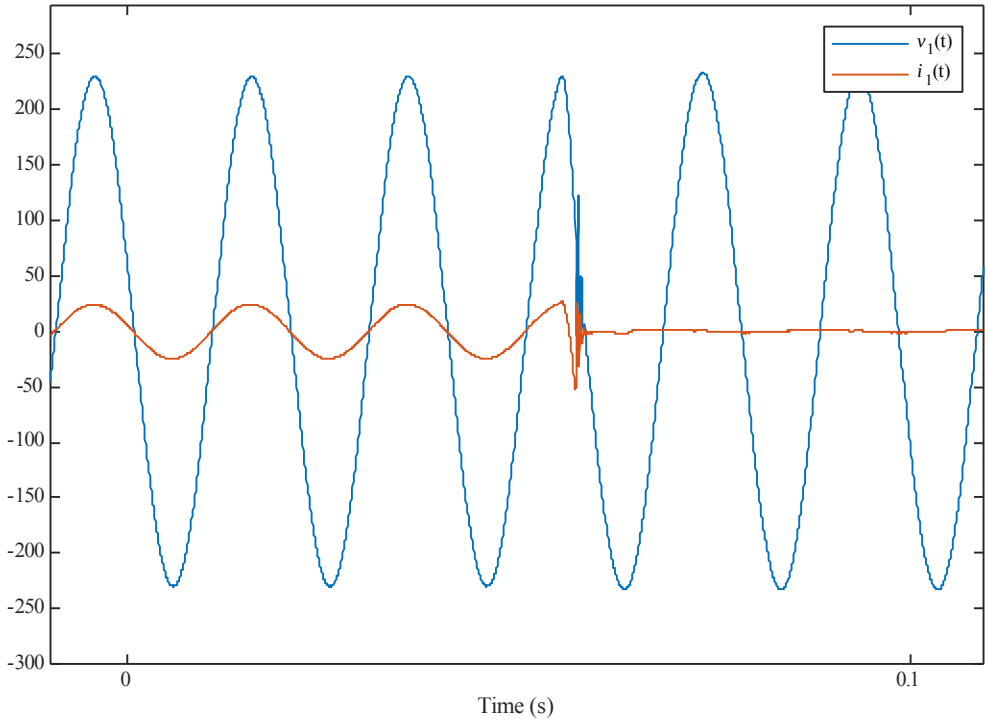
$v_1(t)$
$i_1(t)$
250
200
150
100
50
0
-50
-100
-150
-200
-250
-300
0
0.1
Time (s)

(b)

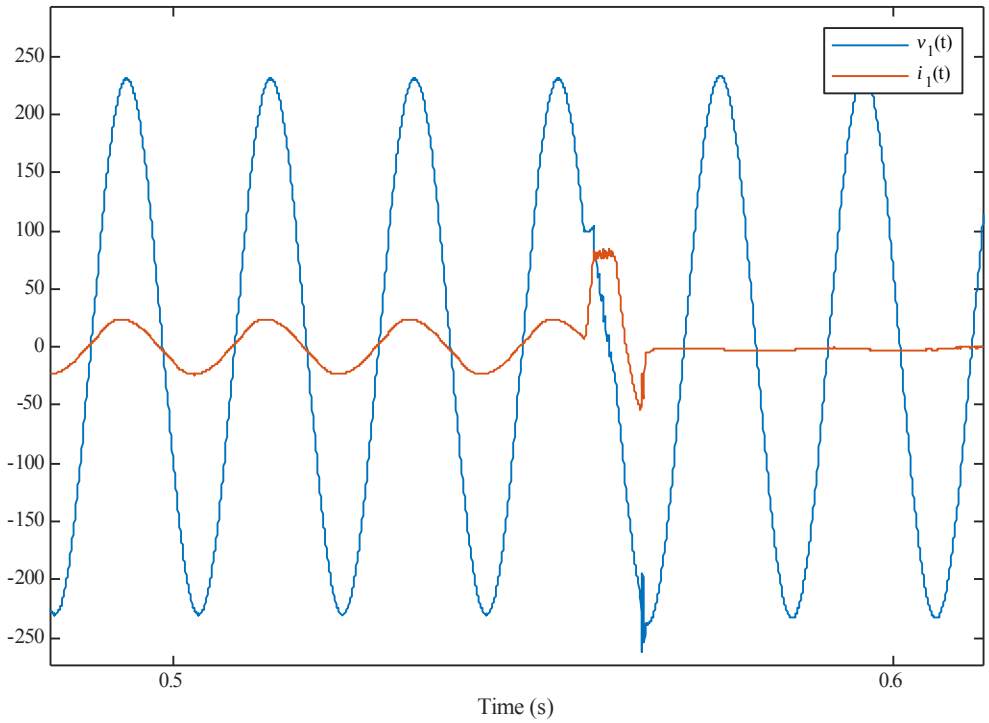


(c)

**Figure 56: Inverter response to phase angle jump/shift of 45° - iteration 7, (rode through).**

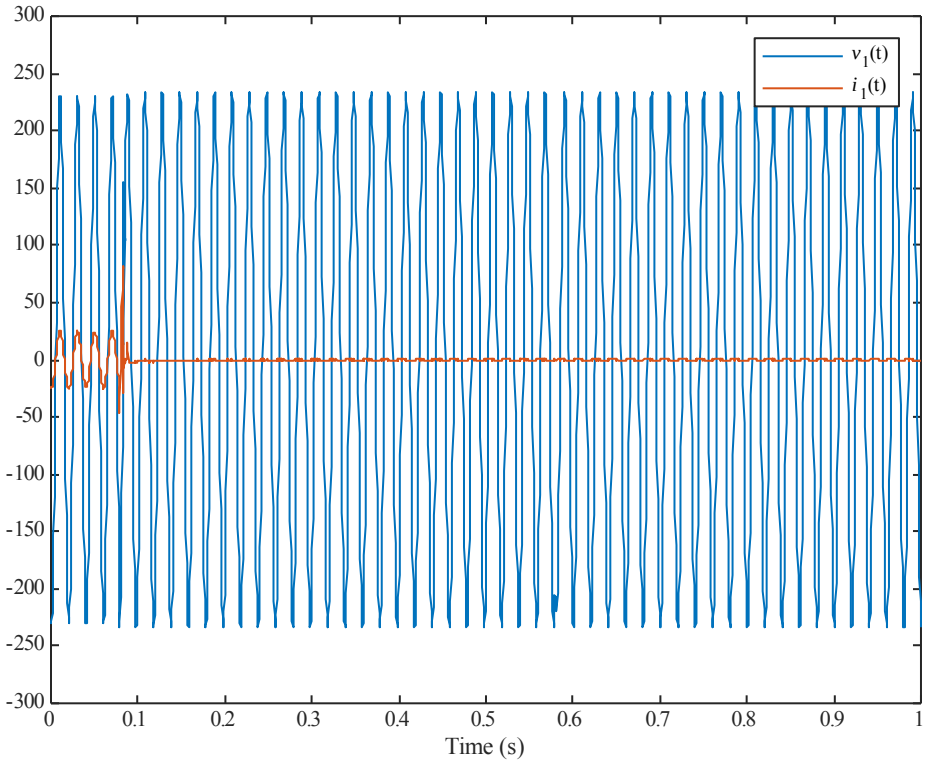


(a)

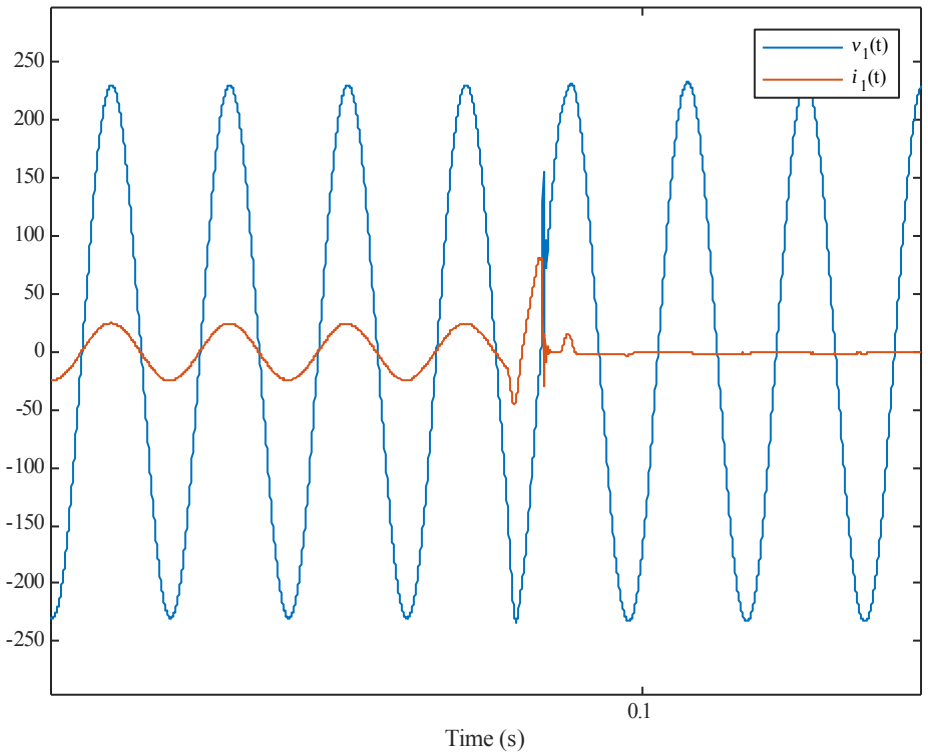


(b)

**Figure 57: Inverter response to phase angle jump/shift of 45° - iteration 8, (disconnected).**

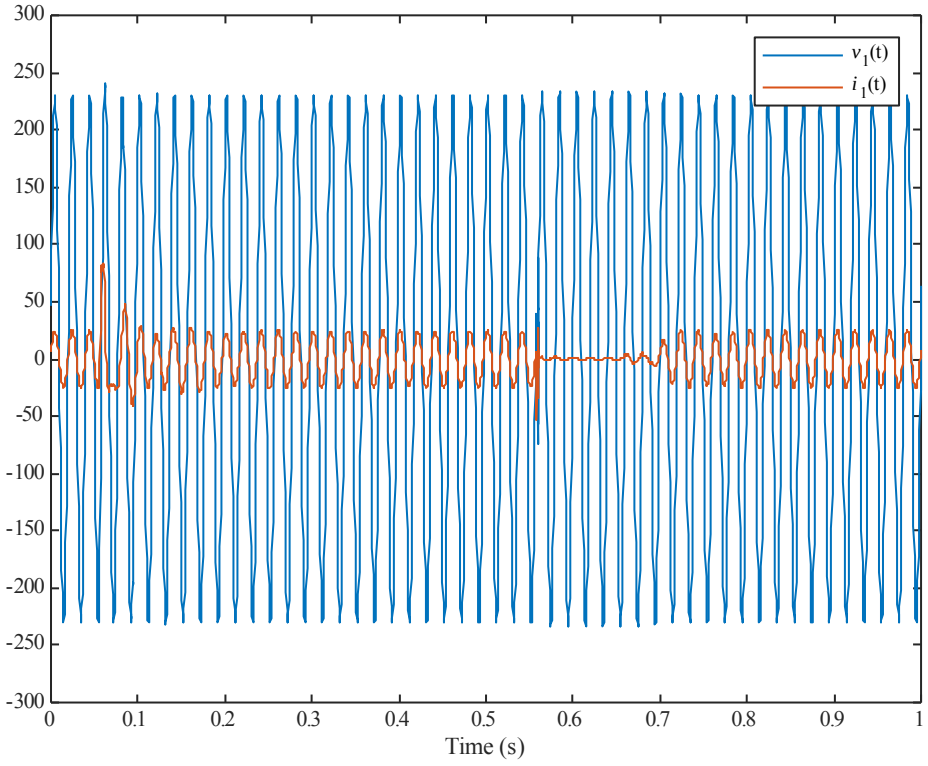


(a)

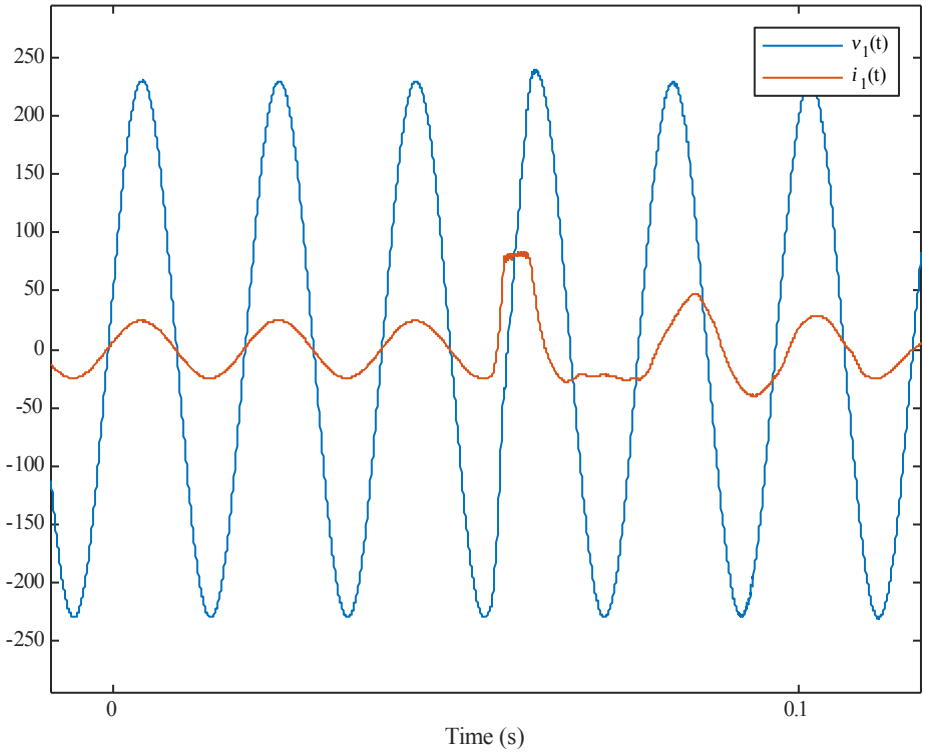


(a)

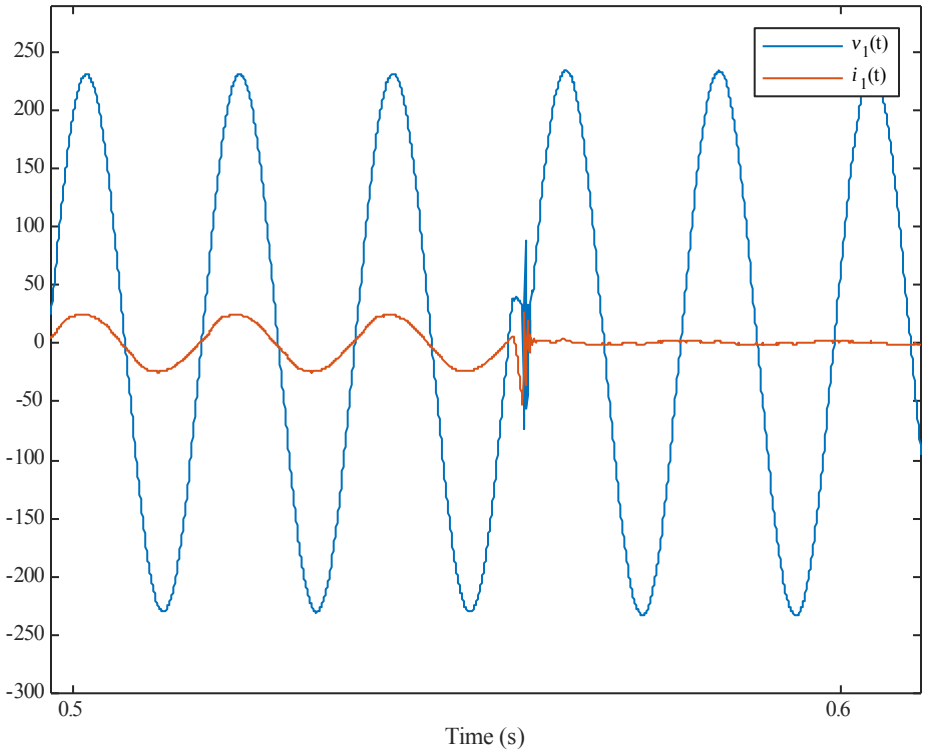


(b)

**Figure 58: Inverter response to phase angle jump/shift of 45° - iteration 9, (rode through).**

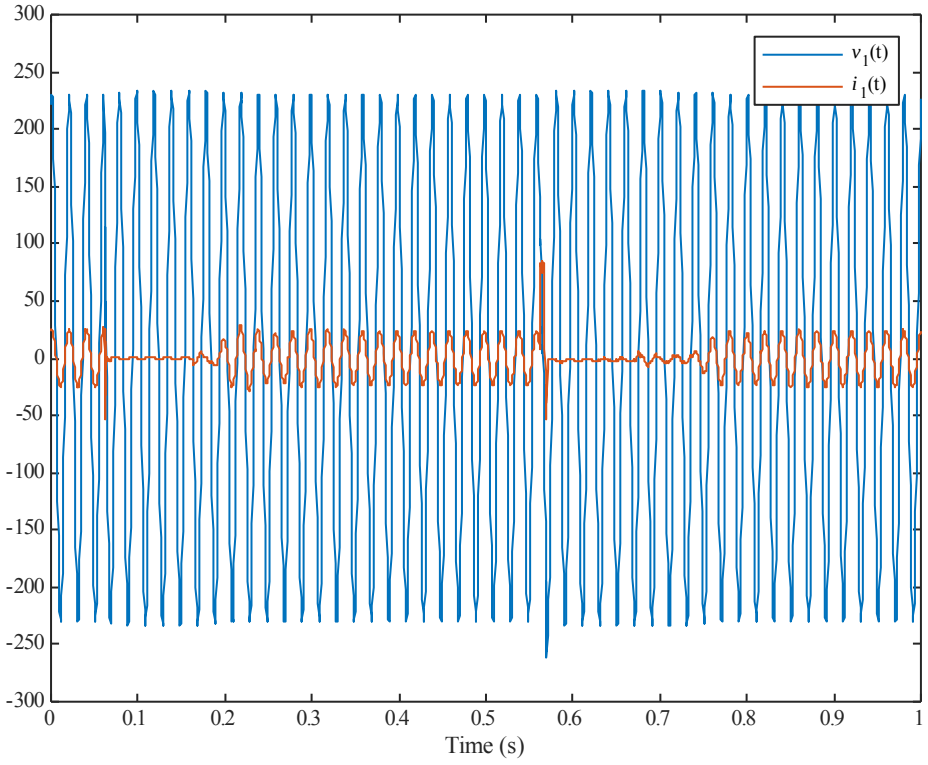
$v_1(t)$
$i_1(t)$
300
250
200
150
100
50
0
-50
-100
-150
-200
-250
-300
0
0.1
0.2
0.3
0.4
0.5
0.6
0.7
0.8
0.9
1
Time (s)

(a)

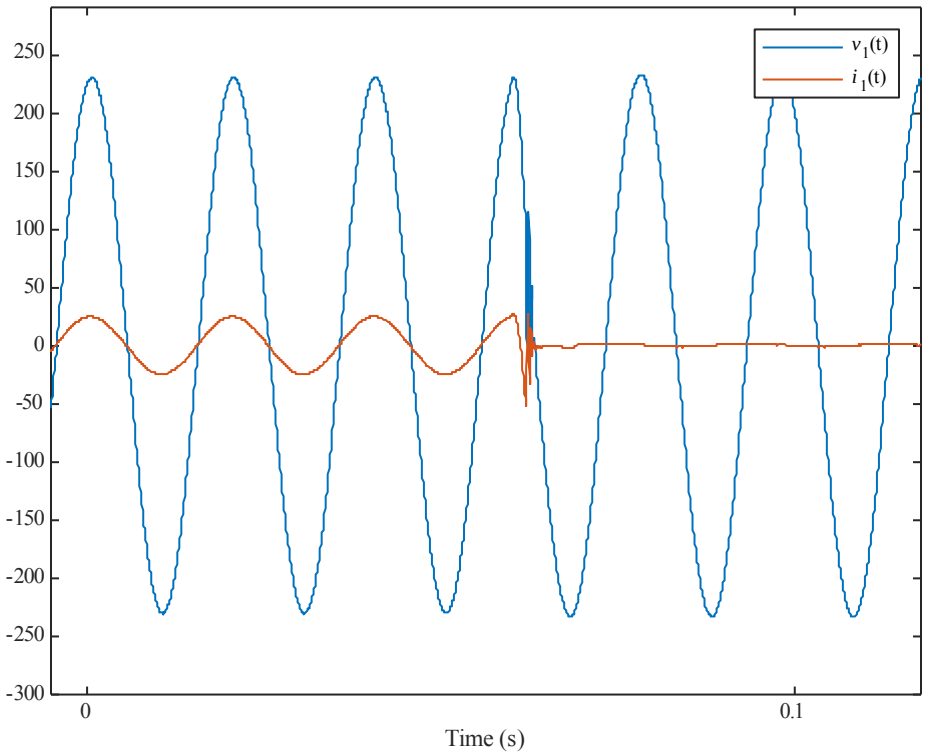
$v_1(t)$
$i_1(t)$
250
200
150
100
50
0
-50
-100
-150
-200
-250
-300
0
0.1
Time (s)

(b)

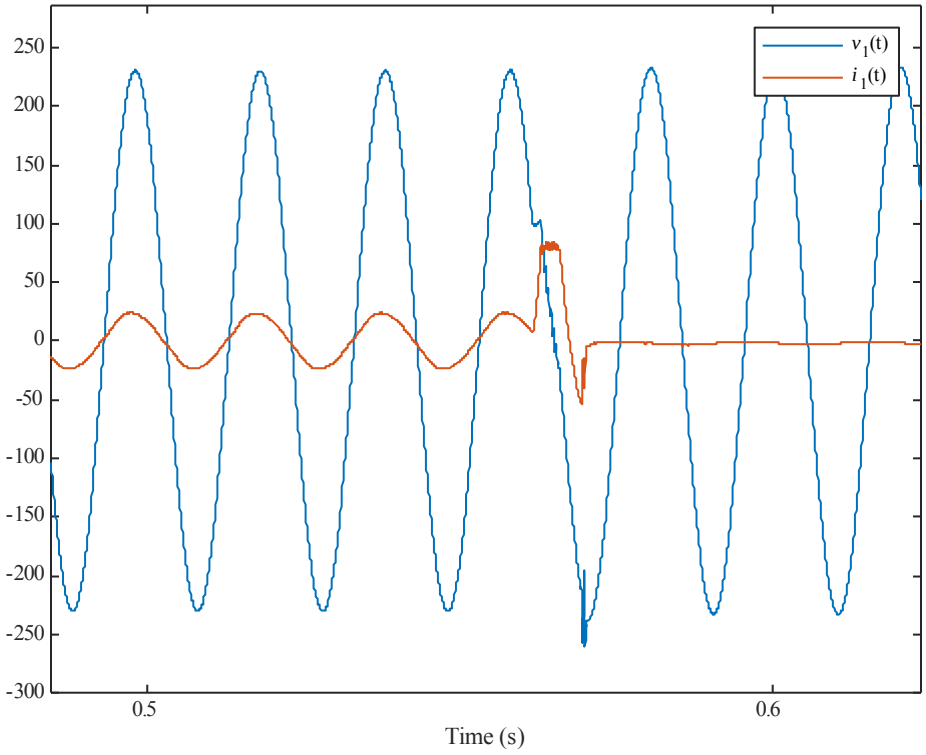


(c)

**Figure 59: Inverter response to phase angle jump/shift of 45° - iteration 10, (rode through).**

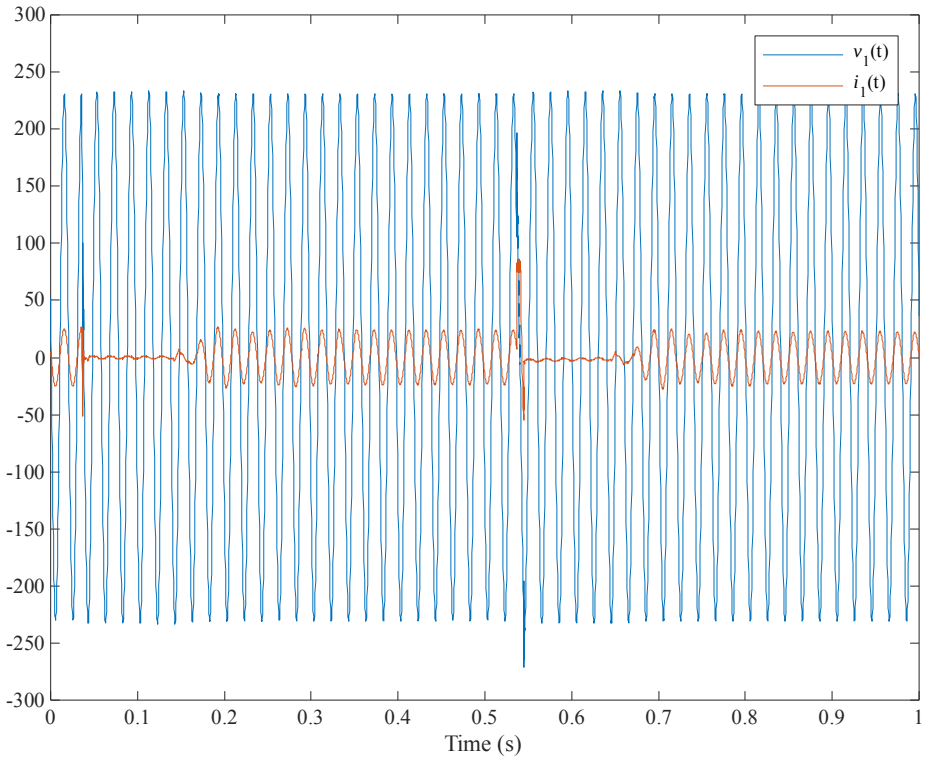


(a)

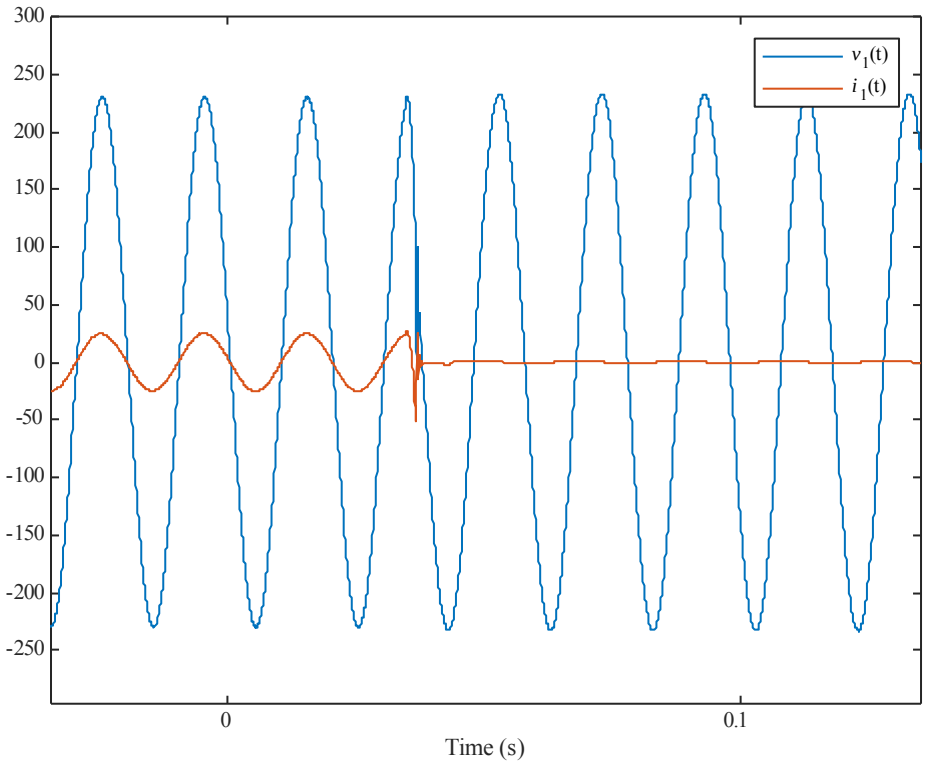


(b)

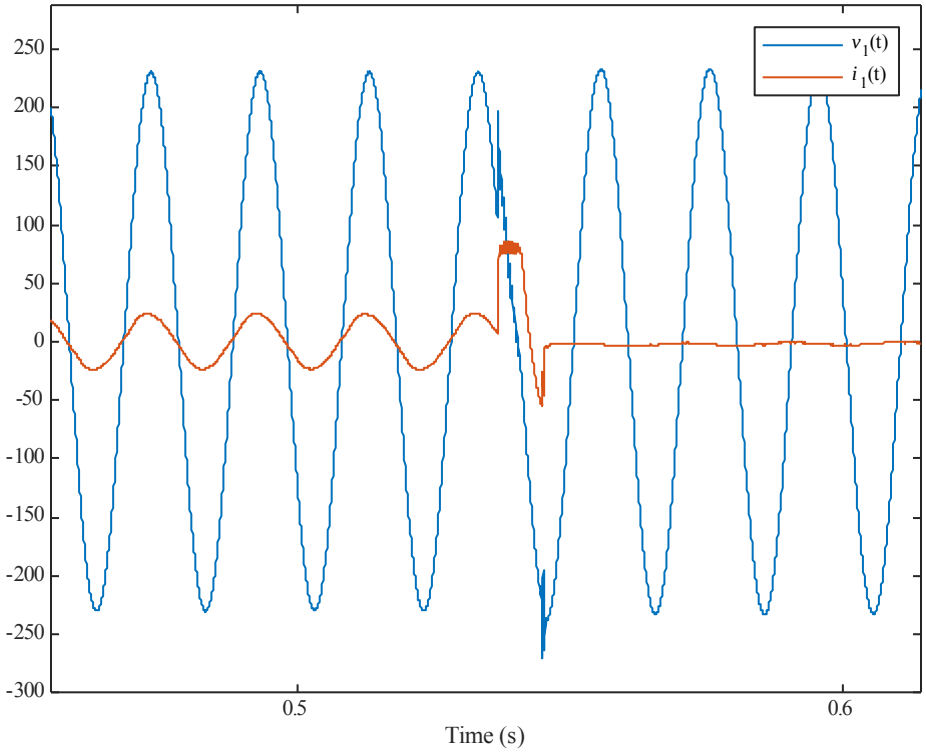


(c)

**Figure 60: Inverter response to phase angle jump/shift of 45° - iteration 11, (rode through).**

## C.4 Test results for additional grid services

### C.4.1 Peak shaving

**Figure 61** and **Figure 62** show that the charger can respond to changing charging/discharging current set-points, thus it is possible to provide peak shaving services for the Wallbox charger.

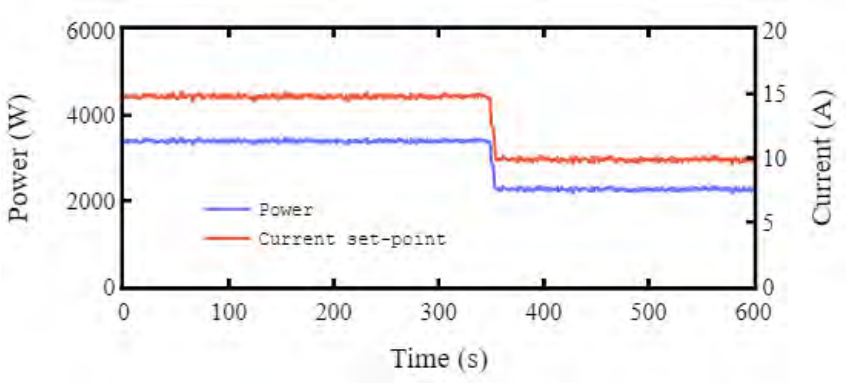


**Figure 61: Active power response to current set point changes from 15 A to 10 A.**

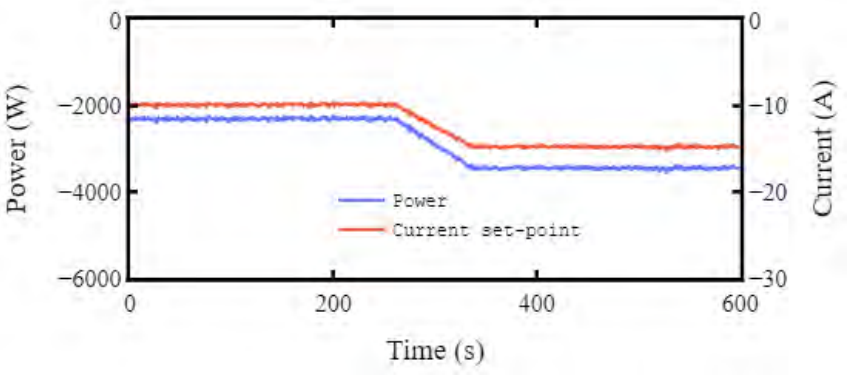


**Figure 62: Active power response to current set point changes from − 15 A to − 10 A.**